

High Accuracy *ab Initio* Calculations of Rotational–Vibrational Levels of the HCN/HNC System

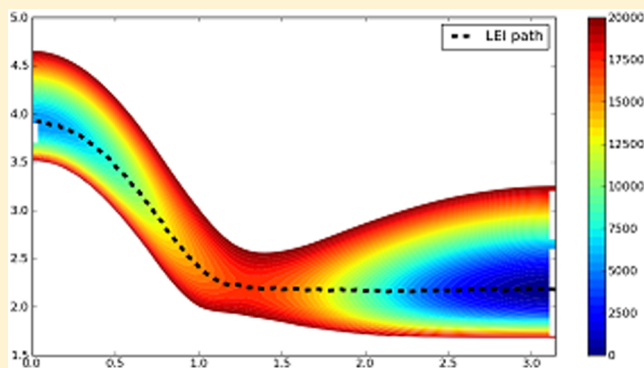
Vladimir Yu. Makhnev,[†] Aleksandra A. Kyuberis,[†] Nikolai F. Zobov,[†] Lorenzo Lodi,[‡] Jonathan Tennyson,[‡] and Oleg L. Polyansky^{*,†,‡}

[†]Institute of Applied Physics, Russian Academy of Science, Ulyanov Street 46, Nizhny Novgorod, Russia 603950

[‡]Department of Physics and Astronomy, University College London, Gower Street, London WC1E 6BT, United Kingdom

S Supporting Information

ABSTRACT: Highly accurate *ab initio* calculations of vibrational and rotational–vibrational energy levels of the HCN/HNC (hydrogen cyanide/hydrogen isocyanide) isomerising system are presented for several isotopologues. All-electron multireference configuration interaction (MRCI) electronic structure calculations were performed using basis sets up to aug-cc-pCV6Z on a grid of 1541 geometries. The *ab initio* energies were used to produce an analytical potential energy surface (PES) describing the two minima simultaneously. An adiabatic Born–Oppenheimer diagonal correction (BODC) correction surface as well as a relativistic correction surface were also calculated. These surfaces were used to compute vibrational and rotational–vibrational energy levels up to 25 000 cm^{−1} which reproduce the extensive set of experimentally known HCN/HNC levels with a root-mean-square deviation $\sigma = 1.5$ cm^{−1}. We studied the effect of nonadiabatic effects by introducing opportune radial and angular corrections to the nuclear kinetic energy operator. Empirical determination of two nonadiabatic parameters results in observed energies up to 7000 cm^{−1} for four HCN isotopologues (HCN, DCN, H¹³CN, and HC¹⁵N) being reproduced with $\sigma = 0.37$ cm^{−1}. The height of the isomerization barrier, the isomerization energy and the dissociation energy were computed using a number of models; our best results are 16 809.4, 5312.8, and 43 729 cm^{−1}, respectively.



1. INTRODUCTION

The HCN/HNC system represents a prototype of isomerization processes and, also for this reason, has been the subject of several high-resolution spectroscopy studies. Baraban et al.¹ and Mellau et al.² recently studied the [H,C,N] system focusing on one important stationary point—the saddle point. Saddle points are related to chemical processes through transition state theory. The [H,C,N] system is an ideal candidate to study quantum eigenstates in the neighborhood of a saddle point.¹ Mellau and co-workers were the first to employ experimental spectroscopic methods as a direct probe of transition states and they proposed a general procedure for studying reaction barriers using the properties of the vibrational levels they determined. Mellau and co-workers based their theoretical analysis on the *ab initio* potential energy surface (PES) of van Mourik et al.;³ however, this surface is not accurate by modern standards—see Harris et al.⁴—and improving it is important for future investigations.

Key parameters in the energetics of the HCN/HNC system are the dissociation energy, the height of the isomerization barrier and the energy to isomerization, that is, the energy difference between the lowest rotation–vibrational states of HCN and HNC. Nguyen et al.⁵ recently suggested that the

energy difference between these states is considerably smaller than the value employed by Barber et al. in their calculation of a recent HCN/HNC line list.⁶ This difference is important for the temperature-dependent equilibrium ratio of the two isomers,⁷ which has been suggested may be used as a thermometer in cool carbon stars.⁸ The dissociation energy conversely appears to be little studied theoretically and has been determined experimentally with rather large uncertainties.^{9,10}

Mellau and co-workers have performed very extensive experimental studies of the vibration–rotation spectra of both HCN^{11–18} and HNC,^{19–23} as well as of some rarer isotopologues.^{14,24} Furthermore, highly excited vibrational states lying between 17 000 and 23 000 cm^{−1} (i.e., well above the barrier to isomerization) have been observed by Lehmann and co-workers.^{25,26}

There is significant astrophysical interest in the HCN system;^{27–30} HCN and HNC are important molecules in the interstellar medium and on comets, where they are observed

Received: October 23, 2017

Revised: December 15, 2017

Published: December 18, 2017

significantly outside equilibrium. They also play an important role in providing opacity in carbon-rich stars.⁸ Indeed, HCN was the first molecule used to demonstrate the dramatic importance of comprehensive line lists on atmospheric models of cool stars.³¹ Since then a number of combined HCN/HNC variational line lists have been computed,^{6,32,33} as well as one for the ¹³C isotopologue.³⁴ Recent applications of one these line lists⁶ suggest that HCN could also be an important constituent of the atmospheres of extra solar planets.³⁵ The original HCN/HNC line lists were based on an *ab initio* treatment of the potential energy surface (PES)^{32,36} and many of the resulting line positions lay tens of wavenumbers away from laboratory measurements. Subsequent line lists aimed at improving their predicted line positions by substituting whenever possible computed energy levels with experimentally derived ones.^{6,33} This procedure is clearly limited by the available experimental data and, furthermore, cannot improve intensity predictions. An improved *ab initio* starting point would therefore be very beneficial.

We recently managed to calculate *ab initio* rotation–vibration energy levels for seven water isotopologues up to 15 000 cm^{−1} with an accuracy of 0.08 cm^{−1}.³⁷ A similar level of accuracy was obtained for the isoelectronic ion H₂F⁺.³⁸ The methodology developed in these studies, and discussed below, has been applied to other small molecules. For example, we computed an *ab initio* PES for NH₃³⁹ which accurately (to 1 cm^{−1}) reproduces the observed energy levels up to unprecedentedly high values of the energy. However, nuclear motion calculations for NH₃ are challenging and contribute significantly to the overall error in computed energy levels. As HCN is so well studied experimentally and has the added interest of the isomerization problem, it provides an excellent system for benchmarking our methods. Furthermore, being a triatomic system, the nuclear motion calculations can be performed to high accuracy and we can use a very similar level of *ab initio* theory as employed for water and H₂F⁺. On the other hand HCN has 14 electrons whereas water, ammonia and H₂F⁺ are all 10 electron systems; HCN has two second-row atoms and serves as a prototype for calculations of many similar systems of interest such as C₂H₂, H₂CO, the HF dimer (HF)₂, and the water dimer (H₂O)₂. A successful extension of our previous water results³⁷ to HCN would give hope that a similar level of accuracy could be obtained for larger systems including those mentioned above, although, of course, at the price of a much-increased computational effort.

There are only a few available PESs which span both the HCN and HNC minima. Apart from the *ab initio* surface of Van Mourik et al.³ mentioned above, Varandas and Rodrigues constructed a many-body expansion PES fitted to the experimental energy levels.⁴⁰ As we will show below, the accuracy of the *ab initio* PES produced in this work is superior to the empirical one of Varandas and Rodrigues. Finally, we should mention the study by Dawes et al.,⁴¹ who computed HCN vibrational frequencies with an accuracy of 3.2 cm^{−1}.

This paper is organized as follows. Section 2 gives the technical details of our *ab initio* calculations and describes the procedure used to fit the points obtained to an appropriate functional form. Section 3 presents the results of nuclear motion calculations using the DVR3D program suite⁴² for vibrational and rotation–vibration levels of HCN; comparisons with the known experimental energy levels are also presented. Section 4 discusses our results and presents our conclusions, putting forward some suggestions for future work.

2. AB INITIO CALCULATIONS

General Approach. We identify 11 components affecting the PES and which can influence rotation–vibrational energy levels by 0.1 cm^{−1} or more. These contributions are discussed in detail in our work on water³⁷ and H₂F⁺.³⁸ Our strategy is similar in spirit to various “model chemistry” schemes used in theoretical thermochemistry⁴³ and to the focal-point analysis,⁴⁴ namely, our approach is based on a main potential energy surface of good quality to which several smaller correction surfaces are added.

In this work we consider the following six components:

- 1 A main surface based on multi reference configuration interaction (MRCI)—possibly in the internally contracted approximation (ic-MRCI)—or closely related methods such as averaged coupled pair functional (ACPF) or averaged quadratic coupled cluster (AQCC). The active space should preferentially be the full-valence complete active space (CAS). A well-known disadvantage of MRCI is that it is not size extensive, which leads to a degradation of its accuracy as the number of electrons in the system grows. However, for small molecules with less than about 15 electrons MRCI-type methods are the most accurate quantum chemistry approaches in widespread use. Furthermore, in practice size extensivity corrections are found to work quite well and they generally improve the quality of MRCI energies. The Molpro package⁴⁵ provides four types of size extensivity corrections to ic-MRCI energies, namely the renormalized Davidson and the Pople correction computed using either the “fixed” or “relaxed” coefficient; see ref 46 and the Molpro manual for an explanation. As we show below, for the bottom of the HCN potential well all these four versions of size-extensivity corrections give very similar results; however, close to the isomerization barrier transforming HCN into HNC and at the bottom of the HNC potential well, the corrections are significantly different.
- 2 Very large basis sets must be used, which in practice translates into the aug-cc-pV6Z and aug-cc-pV5Z basis sets of Dunning with basis-set extrapolation. Basis sets of 7- ζ quality (or even larger) or explicitly correlated calculations of the F12 type would also be very beneficial.
- 3 A dense grid of points must be used. Calculations on H₃⁺ showed⁴⁷ that using a small, 69-point grid⁴⁸ in this highly symmetrical system led to a loss of accuracy of about 0.02 cm^{−1} in rotation–vibrational energy levels when compared with calculations performed on a much denser grid. Furthermore, some 20% of points in the dense grid lay more than 5 cm^{−1}, and sometimes 20 cm^{−1}, away from the value predicted by the 69-point PES. In this case this error is 3 orders of magnitude larger than the intrinsic accuracy of the *ab initio* calculations. Thus, the number of points used to build the PES of a triatomic molecules should be of the order of a few thousands rather than a few hundreds to avoid interpolation artifacts.
- 4 Standard MRCI calculations based on the full-valence CAS are not accurate to the 0.1 cm^{−1} level, and corrections for the incomplete electron-correlation treatment should be computed (see also the discussion below); in practice this means MRCI calculations using larger active spaces and the largest basis set one can

afford. Benchmark calculations with small basis sets and high-order coupled cluster (CCSDTQP if possible) may be used for calibration of the CAS.

- 5 Our experience shows that the shift in the energy levels due to the BODC can be more than 1 cm^{-1} , so that inclusion of a BODC surface is necessary.
- 6 A surface accounting for scalar-relativistic effects should be computed at the MRCI level using either the expectation value of the Pauli Hamiltonian giving the MVD1 (mass-velocity, one-electron Darwin terms) correction or, alternatively, included in the main calculation using the Douglas–Kross–Hess Hamiltonian. A discussion of these relativistic corrections has been given by Tarczay et al.⁴⁹

Consideration of effects due to higher-level relativistic corrections, quantum electrodynamics (QED) and spin–orbit coupling are left to future work. The first of these two effects have been found to be important for water,^{49,50} while spin–orbit effects are likely to be important only near dissociation as HCN is a closed shell system. Neglect of these effects implies that our treatment of HCN cannot possibly reach the 0.1 cm^{-1} level of accuracy. Furthermore, we have not attempted a full *ab initio* treatment of vibrational or rotational nonadiabatic effects (see Discussion).

Our use of ic-MRCI as the starting point instead of single-reference methods such as coupled cluster is conditioned by our aim to create a global PES capable of describing rotational–vibrational spectra as well as isomerization and dissociation. It is well-known that coupled cluster methods are not suitable for describing bond-breaking (unless very high orders of excitations are included, which is usually computationally unfeasible); this makes MRCI the method of choice. Multireference methods such as MRCI require the specification of an “active space”, a set of occupied and virtual orbitals which play an active part in the process considered.⁴⁶ If no restrictions are placed on the occupation numbers of orbitals in the active space, it is called “complete active space” (CAS). The choice of the CAS is an important one, as the accuracy of the results crucially depend on it. A usually good choice is the so-called “full-valence” CAS, which included all valence orbitals (i.e., orbitals which in the dissociation limit correlated with atomic valence orbitals); this is also the default choice of CAS made by Molpro. For molecules with more than about 5 atoms the full-valence active space is usually too expensive to be viable and strategies must be devised to reduce it;^{51,52} on the other hand, when aiming at the highest possible accuracy, for small molecules, MRCI calculations based on the full-valence CAS fall short of the desired accuracy. For water, we showed³⁷ that extending the active space from the full-valence choice led to MRCI calculations at dissociation very close to the highly accurate, but very expensive, coupled-clusters calculations with explicit inclusion of pentuple (5-fold) excitations (CCSDTQP). We also showed that MRCI calculations with this extended CAS gave a very accurate BO surface in the vicinity of equilibrium. Of course, the accuracy of this surface can only be demonstrated once relativistic and beyond-BO corrections are considered.

Details of the Calculation. We performed *ab initio* calculations on the HCN/HNC system at 1541 grid points spanning energies up to $25\,000\text{ cm}^{-1}$. Experimental rotation–vibrational energy levels are available up to $20\,000\text{ cm}^{-1}$ for this system, which allows the surface to be calibrated over an

extended energy range. Calculations were performed with the aug-cc-pwCVSZ and the aug-cc-pCV6Z basis set and all electrons were correlated, as previous experience has shown that all-electron calculations are preferable to frozen-core one complemented by a core–valence correction calculated in a smaller basis set.

As discussed in point 4. above, the standard choice of the full-valence CAS is usually insufficient to give results of the highest accuracy. Specifically, for HCN the full-valence CAS (Molpro’s default choice) corresponds to keeping doubly occupied the C and N 1s core electrons and allowing the remaining 10 valence electrons to occupy freely the 9 valence orbitals, namely 7 a' orbitals and 2 a'' orbitals (C_s labels; at the equilibrium, linear, geometry 5 valence orbitals have symmetry a_1 , 2 symmetry b_1 and 2 symmetry b_2). With respect to water, bonding in HCN and HNC is more complicated, particularly due to the triple $\text{N}\equiv\text{C}$ bond. This is borne out by MRCI calculations in the cc-pVDZ basis set, which show that in the MRCI wave function expansion the weight (=squared expansion coefficient, expressed as a percentage) of the closed-shell Hartree–Fock configuration $(1\sigma)^2(2\sigma)^2(3\sigma)^2(4\sigma)^2(5\sigma)^2(1\pi)^4$ is only 87%, with three more configurations contributing about 1.5% each (the same numbers hold also for HNC). For comparison, in water the Hartree–Fock configuration at equilibrium has a weight of about 95% in MRCI expansion, in H_2F^+ 96% and in ammonia 93%. These numbers indicate that HCN and HNC have, even at equilibrium, a moderate multireference character and therefore one might generally expect a lower accuracy in the treatment of electron correlation than the one achievable for molecules with simpler bonds. During a preliminary phase of this work we produced a PES based on MRCI in the full-valence CAS and the aug-cc-pCV6Z basis set. As expected, this preliminary PES resulted in quite large differences between computed and observed energy levels—the largest deviation for levels up to 7000 cm^{-1} was 26 cm^{-1} for the second overtone of the CH stretch, the (200) level.

We performed further tests to ascertain whether the use of a larger CAS might give better results. These experimentations proceeded on two fronts. On one side we computed reference, near full configuration interaction (FCI) *ab initio* energies with the small cc-pVDZ and compared our reference curves with curves obtained with MRCI (possibly complemented with the renormalized Davidson or Pople size-extensivity corrections) using several choices of CAS, with a view to selecting the CAS which best reproduces the reference energies. This small study, discussed below, was, however, rather inconclusive. On the other side we computed PESes for the bottom of the HCN well using MRCI and several choices for the CAS in the aug-cc-pVQZ basis set (frozen core calculations) and then computed energy levels for HCN using our 6- ζ PES supplemented with the difference between the 4- ζ full-valence PES and the one in our trial CAS. We then compared computed energy levels with experiment. This approach, also discussed below, led to our final choice of a CAS including one extra a' orbital, which was then used for all calculations presented in this work.

Choice of the CAS by Comparison with High Order Coupled Cluster. In our comparison against “near FCI” results we considered stretches of the CH and the CN bond up to about $10\,000\text{ cm}^{-1}$ from equilibrium (the other bond and the bond angle were kept fixed at their equilibrium values); we did not consider bends partially because calculations for nonlinear geometries take longer because of the reduction in symmetry.

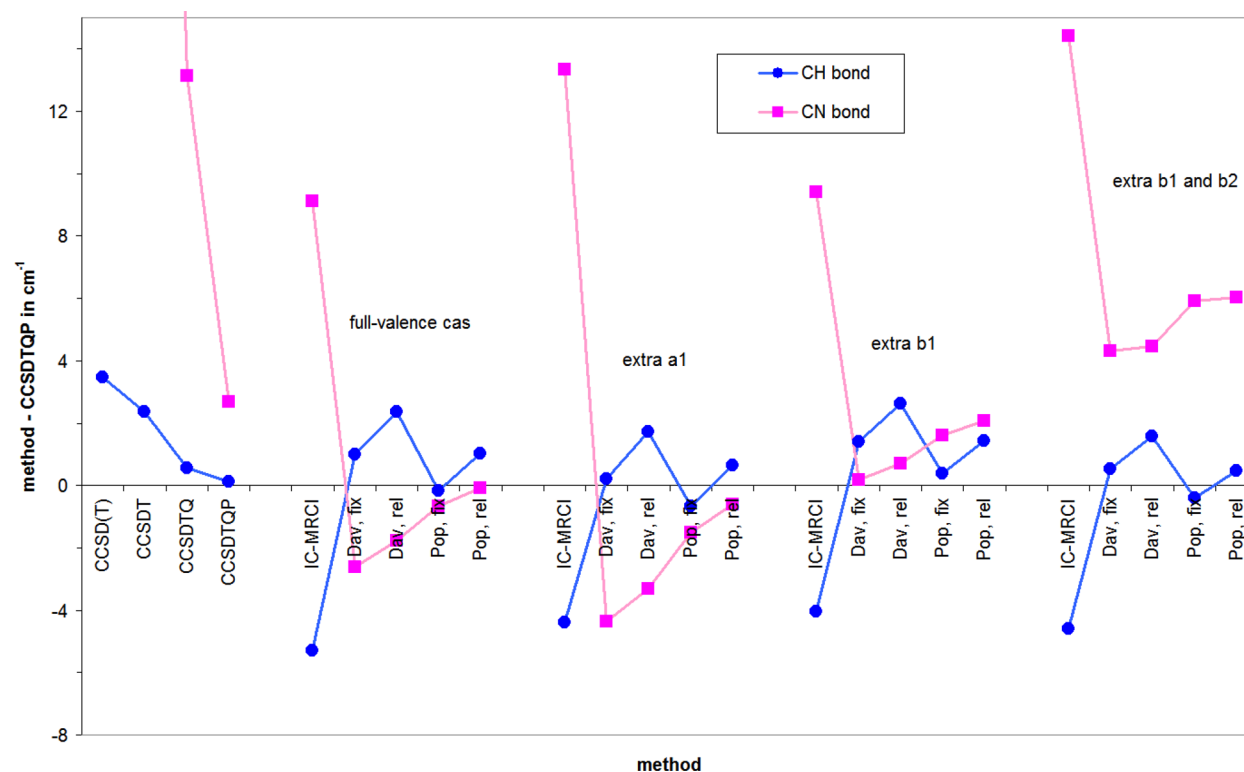


Figure 1. Estimated errors with respect to FCI in the cc-pVDZ for various levels of coupled theory (on the left) and MRCI with various choices for the CAS (see text). Errors refer to the $\nu = 0$ to $\nu = 2$ transition for CH stretch keeping the NC bond fixed (blue dots; the estimated FCI value is 8093.75 cm^{-1}) and for the NC stretch keeping the CH bond fixed (magenta squares; the estimated FCI value is 7452.44 cm^{-1}). See text for details.

CCSDTQP/cc-pVDZ calculations took about 10 h per point on a workstation with a quad-core Intel i7-3770 CPU. FCI calculations of HCN in this basis set are within the realm of possibility but require, using Molpro, 60 GB of ram, which is more than we have at our disposal on our machine. As reference energies, we therefore extrapolated the CCSDTQ and CCSDTQP energies assuming an exponential convergence with respect to the level of excitations included.

The comparison of our MRCI curves to the reference one was carried out by looking at average differences and at the nonparallelity error (NPE, defined as the difference between the maximum difference and the minimum difference of the two curves) as well as by computing diatomic-like vibrational energy levels for the two stretches and examining the differences in the computed energy levels. Specifically, we considered three CASes larger than the full-valence one obtained, respectively, by adding to it one extra virtual orbital of symmetry a_1 , by adding one extra orbital of symmetry b_1 (adding one b_2 orbital yields the same results) or by adding one b_1 and one b_2 orbital. We provide a spreadsheet with these tests and more details; an indicative plot is reported as Figure 1.

Here is a brief summary of the conclusions from this test. For the H–CN single bond stretch we considered the discrepancy in the $\nu = 0$ to $\nu = 2$ vibrational transition, which has energy 8093.75 cm^{-1} using our extrapolated FCI curve (atomic masses for C and H were used). As one can see from Figure 1 the coupled cluster hierarchy converges rather quickly to the FCI limit; the RHF curve is error by 379.12 cm^{-1} , CCSD by 48.69 cm^{-1} , CCSD(T) by 3.47 cm^{-1} , CCSDT by 2.36 cm^{-1} , CCSDTQ by 0.57 cm^{-1} , and CCSDTQP by an estimated 0.14 cm^{-1} . MRCI does well but not exceptionally so in this test. All four CASes considered gave similar results. Uncorrected

MRCI is in error by about 5 cm^{-1} . The four size extensivity corrected (SEC) MRCI values reduce the MRCI error by a factor about 7 for all CASes and are clustered together within 0.8 cm^{-1} , which value can be taken as an indication of their error. In summary in this test SEC MRCI performs at a level of accuracy intermediate between CCSDT and CCSDTQ, and none of the extended CAS considered appears to be significantly better than the full valence one.

For the HC–N triple bond stretch we considered the discrepancy in the $\nu = 0$ to $\nu = 3$ vibrational transition, which has energy 7448.92 cm^{-1} using our extrapolated FCI curve (atomic masses for C and N were used). It is well-known that for coupled cluster triple bond breaking is exceedingly difficult to describe^{53,54} and that even including up to hexuple (6-fold) excitations is not enough to describe such a bond breaking process up to dissociation.⁵⁵ Such difficulties are evident from Figure 1. In this case CCSD is error by 236.44 cm^{-1} , CCSD(T) by 39.79 cm^{-1} , CCSDT by 58.66 cm^{-1} , CCSDTQ by 13.13 cm^{-1} , and CCSDTQP by an estimated 2.69 cm^{-1} . The large estimated error of CCSDTQP raises some concerns on the quality of our extrapolated FCI curve; in future studies instead of coupled cluster it would be beneficial to use some of the modern alternative approaches to obtain “near FCI” reference curves,^{55–61} but this strategy was not pursued at this time. The four CASes lead to broadly similar results, although the two CAS including extra b_1 or b_2 orbitals seem to systematically underestimate the value of the considered transition. With respect to the reference value uncorrected MRCI energy levels are off by about 12 cm^{-1} , while SEC values by about 2.5 cm^{-1} , which is also approximately the scatter between them.

In summary the only reasonably certain conclusion of our small study is that MRCI SEC energies are better than

uncorrected MRCI ones. The four CASes considered lead to similar results, although there is weak evidence that the full-valence CAS and the one obtained adding one extra a_1 orbital perform somewhat better for the CN stretch. The main limitation in this study lies in the smallness of the cc-pVDZ basis set, as the agreement of methods with respect to FCI may be different in the large basis set limit.

Choice of the CAS by Comparison with Experiment. As a consequence of the limitations of the study detailed above we decided to use a more pragmatic approach in which the choice of the CAS was dictated by best agreement with experiment. As outlined in the previous section, we investigated the effect of extended CASes by computing in the aug-cc-pVQZ basis set the differences between energies in the full-valence CAS and the trial one and then used this difference as a correction surface to our 6ζ full-valence PES. These tests indicated that best agreement with experiment was obtained with MRCI+P-r energies (Pople correction, relaxed reference) in the CAS obtained by adding an extra a' orbital. We therefore used this PES for our further investigations.

Our procedure may raise some perplexities as it relies, to an extent, on fortuitous coincidence of one particular methods with experiment and it can be accused of getting 'the right result for the wrong reason'. While such concerns would not be unreasonable in other contexts, we would like to stress that this work is not a study of quantum chemical methods; the goal of this work is to produce new *ab initio* PESes for the HCN/HNC system which (i) reproduce to high accuracy the existing experimental data and (ii) are capable of predicting unmeasured energy levels and transitions with comparable accuracy. As we will show in the following, we believe this goal has been largely achieved.

HCN/HNC Global PES. As detailed in the previous section the main component of our HCN/HNC global PES is based on MRCI+P-r energies (MRCI with Pople correction, relaxed reference) in the aug-cc-pCV6Z basis set. The first column of Table 2 gives the resulting differences between observed and calculated (obs-calc) energy levels for this BO calculation (details on the nuclear motion calculations are given in the next section). This level of theory, supplemented with new BODC and scalar-relativistic correction surfaces (detailed below), was used to create our global PES of the HCN/HNC system.

Basis Set Extrapolation. HCN-Only PES. We also computed a separate PES for the low-energy legion of the HCN well based this time on Davidson "fixed reference" (MRCI+Q-f) energies and including complete basis set (CBS) extrapolation, with the Davidson fixed size-extensivity correction. For basis set extrapolation we used the 2-point formula based on the aug-cc-pwCVSZ and aug-cc-pCV6Z ($n = 5$ and 6) basis sets, originally suggested by Martin:⁶²

$$E_n = E_{\text{CBS}} + \frac{A}{\left(n + \frac{1}{2}\right)^4} \quad (1)$$

which leads to the extrapolation formula

$$E_{\text{CBS}} = E_6 + F_6(E_6 - E_5) \quad (2)$$

where $F_6 = 14641/13920 = 1.051795977$ is an extrapolation coefficient. This extrapolation was shown to work very well in our previous study on H_2F^{+38} and is also a good choice for the calculation of atomization energies, ionization potentials and electron affinities.^{63–65}

Fitting the *ab Initio* Points. We first attempted to fit a set of 1050 *ab initio* points describing the HCN potential well using a polynomial form in the coordinates r_{CH} , r_{CN} , and θ , the HCN angle. The highest power used was 6, the number of constants 7, and the resulting standard deviation was 0.45 cm^{-1} . However, when we used this PES to calculate vibrational energy levels, all the states involving ν_1 vibrational excitations produced a relatively large deviation from experiment, of the order of 3 cm^{-1} .

Using a similar polynomial functional form for the HNC well did not result in a satisfactory PES either. These two factors led us to abandon polynomial fits of the separate HCN and HNC wells; instead we concentrated on a global fit of the HCN/HNC PES, as done by Van Mourik et al.³

The functional form of Van Mourik et al. was used to give an analytic representation of the BO PES:

$$V(r, R, \gamma) = \sum_{i,j,k} A_{ijk} X^i(R, r, \gamma) Y^j(r, \gamma) P^k(\cos \gamma) \quad (3)$$

where r is the CN distance, R is the (H–center-of-mass of CN) distance and γ is the angle between r and R , measured in radians, with $\gamma = 0$ corresponding to HNC and $\gamma = \pi$ to HCN. X and Y are Morse-like coordinates given by

$$X(R, r, \gamma) = 1 - e^{-\alpha_R(\gamma)[R - R_e(\gamma, r)]} \quad (4)$$

$$Y(r, \gamma) = 1 - e^{-\alpha_r[r - r_e(\gamma)]} \quad (5)$$

More details on the functional form are given by Van Mourik et al.³ Altogether 277 PES parameters were determined from the fit of 1541 aug-cc-pCV6Z *ab initio* points.

During fitting we realized that points for near-linear configurations (γ between 0 and 7°) were off by about 96 cm^{-1} from the value estimated from the rest of the points; this was due to incorrect convergence of the complete active space self-consistent field (CASSCF) wave function because of orbital degeneracies at linearity. This problem was solved very simply by adding an extra restricted Hartree–Fock (RHF) calculation prior to CASSCF one. The final fit gave a standard fitting deviation for the 1541 points of the global HCN/HNC PES of 2.6 cm^{-1} . The resulting aug-cc-pCV6Z ic-MRCI PES provides the BO surface for all our global calculations and will be referred to as our global PES below.

Fit of the Correction Surfaces. Scalar-relativistic corrections were computed at the MVD1 (mass-velocity plus one-electron Darwin) level using Molpro as a part of MRCI calculations using the same basis set. Scalar-relativistic effects constitute the largest correction to our BO PES. The relative difference between the smallest and largest relativistic correction is about 25 cm^{-1} . Our relativistic surface was fitted separately to the form

$$V_{\text{MVD1}}(r_1, r_2, \theta) = \sum_{i,j,k} K_{ijk} r_1^i r_2^j \cos^k \theta \quad (6)$$

where r_1 , r_2 and θ are the valence coordinates

$$r_1 = r_{\text{CH}}, r_2 = r_{\text{CN}}, \theta = \widehat{\text{HCN}} \quad (7)$$

The fit uses 34 parameters. This surface reproduces our computed points with a root-mean-square fitting deviation 0.01 cm^{-1} .

The BODC PES was computed using the CFOUR suite⁶⁶ and is based on CCSD valence-only calculations in the aug-cc-pVTZ basis set. The fit of the BODC points was made using

Table 1. Input Parameters for the DVR3DRJZ Module of DVR3D⁴² (Morse Parameters in Atomic Units)

parameter	value	description
NPNT1	40	no. of r_1 radial DVR points (Gauss–Laguerre)
NPNT2	40	no. of r_2 radial DVR points (Gauss–Laguerre)
NALF	50	no. of angular DVR points (Gauss–Laguerre)
NEVAL	950	no. of eigenvalues/eigenvectors required
MAX3D	2500	dimension of final Hamiltonian
XMASS (H)	1.007825; 1.007276 Da	mass of the hydrogen atom ^a
XMASS (C)	12.000000; 11.996707 Da	mass of the carbon atom ^a
XMASS (N)	14.003074; 13.999232 Da	mass of the nitrogen atom ^a
r_{1e}	2.3	Morse parameter (r_1 radial basis function)
D_{1e}	0.1	Morse parameter (r_1 radial basis function)
ω_{1e}	0.0105	Morse parameter (r_1 radial basis function)
r_{2e}	3.2	Morse parameter (r_2 radial basis function)
D_{2e}	0.1	Morse parameter (r_2 radial basis function)
ω_{2e}	0.004	Morse parameter (r_2 radial basis function)

^aRespectively: atomic masses; nuclear masses.

the functional form given by eq 6. The standard deviation of the fit was 0.1 cm^{−1}.

The adiabatic BODC correction leads to shifts in the PES between −0.8 and −6.5 cm^{−1} and always leads to a lowering of the rotation–vibrational energy levels by approximately 1.2 cm^{−1} for each vibrational quanta.

Separate Fit of the HCN Potential Well. The form 3 was used to fit the second PES, representing only the HCN potential well. In this case we carried out basis set extrapolation using formula 1 of MRCI+Q-f energies for about 1000 geometries describing the HCN potential. The root-mean-square fitting deviation is $\sigma = 1.4$ cm^{−1}. This PES will be referred to as the HCN-only PES.

3. NUCLEAR MOTION CALCULATIONS

Vibrational energy levels were calculated using the DVR3D program suite.⁴² The parameters used are presented in Table 1; Morse oscillators-like functions were used for the radial basis functions.

DVR3D offers two choices of internal coordinates for solving the nuclear motion problem, namely Jacobi (scattering) coordinates or Radau coordinates; with adequately large basis sets either choice would give the same result. We performed tests with both Radau (with N as the central atom) and Jacobi coordinates; differences between Jacobi and Radau coordinates calculations were less than 0.01 cm^{−1} for levels below 10 000 cm^{−1} and up to 0.06 cm^{−1} for levels up to 16 000 cm^{−1}, so either coordinates provide sufficient accuracy. An advantage of Radau coordinates is that DVR3D for this choice implements⁶⁷ diagonal nonadiabatic corrections of the type introduced by Schwenke.⁶⁸ Such corrections have been used both for our *ab initio* water energy level calculations³⁷ and for deriving a spectroscopically determined PESs for water.^{69,70} For this reason we used Radau coordinates for all the nuclear-motion calculations.

Nonadiabatic Corrections. Studies on several molecules have shown that nonadiabatic corrections may be as large as a few cm^{−1} for energy levels around 10 000 cm^{−1} (see, e.g., Table 3 of ref 71)), so that they must be taken into account in high-accuracy studies. Fortunately, a great part of the nonadiabatic shifts (with respect to the rotation–vibration energy levels obtained using nuclear masses) can be taken into account very simply by using atomic instead of nuclear masses or, by allowing for the introduction of a small empirical element, by

treating masses as free parameters to be fixed by accurate reference data. At a further level of sophistication, it is now well understood that nonadiabatic shifts can be accurately modeled by a modification of the nuclear kinetic energy Hamiltonian, which may be interpreted as introducing position-dependent masses.^{68,71–74}

We modeled the nonadiabatic effects in HCN using both the approaches outlines above. Initially, as suggested above, we very simply repeated the nuclear-motion calculations using atomic masses instead of nuclear ones; this modification allows for between 50 and 90% of our estimated (see below) vibrational nonadiabatic shifts and gives results which are significantly more accurate than those obtained using nuclear masses.

Subsequently we also tried a more sophisticated method originally developed by Schwenke.⁶⁸ In its simplest version this method consists in adding corrections to the kinetic energy operator in the nuclear-motion Hamiltonian. For the water molecule Schwenke calculated the nonadiabatic corrections and fitted the results of these calculations to a small set of nonadiabatic constants. Only two of them contribute significantly to the energy levels and they have been used in ref 37 to obtain very accurate energy levels. We programmed these two corrections for our HCN/HNC calculations using the functional forms

$$\Delta H_{\text{radial}}^{\text{NBO}} = -\frac{\partial}{\partial r_1} a \frac{\partial}{\partial r_1} \quad (8)$$

$$\Delta H_{\text{angular}}^{\text{NBO}} = -\frac{\partial}{\partial \theta} b \frac{\partial}{\partial \theta} \quad (9)$$

For reference, Schwenke⁶⁸ calculated *ab initio* for H₂O $a = 1.03 \times 10^{-7}$ a.u. and $b = 1.41 \times 10^{-8}$ a.u., although in ref 37 we found it necessary to rescale them by a factor of 1.37 to obtain best agreement with experiment.

For HCN molecule there are no such *ab initio* calculations available, so we determined the a and b parameters empirically by optimizing the calculated $J = 0$ energy levels of HCN and DCN for that they reproduce the experimental ones. For HCN we obtained values $a = 1.27 \times 10^{-7}$ a.u. and $b = 3.0 \times 10^{-8}$ a.u.. As detailed below, although we used only the HCN and DCN isotopologues to determine the constants we obtained almost the same level of agreement with experiment for the levels also for H¹³CN and HC¹⁵N. For H₂O these parameters were

Table 2. H¹²C¹⁴N Vibrational Band Origins Calculated Using the HCN-Only PES and Atomic Masses^a

ν_1	ν_2	ν_3	obs	obs – calc				
				BO	+ad + rel	+NBO	Var. and Rod.	VanMour.
0	2	0	1411.42	−0.27	−0.15	0.05	0.03	−3.50
0	0	1	2096.85	0.06	0.41	0.15	−0.27	−3.73
0	4	0	2802.96	−0.52	−0.20	0.20	0.94	1.50
1	0	0	3311.48	−1.89	−1.41	−0.18	−2.24	3.74
0	2	1	3502.12	−0.58	−0.12	−0.18	−0.77	−8.87
0	0	2	4173.07	−0.09	0.61	0.10	−0.12	−3.17
0	6	0	4174.61	−1.33	−0.70	−0.10	1.76	−6.84
1	2	0	4684.31	−2.72	−2.15	−0.73	−1.65	−1.97
0	4	1	4888.00	−0.67	−0.01	0.12	−1.30	−3.76
1	0	1	5393.70	−1.94	−1.09	−0.10	0.01	−0.73
0	8	0	5525.81	−1.78	−0.78	0.01	1.19	−11.95
0	2	2	5571.89	−0.75	0.07	−0.26	−0.07	−14.61
1	4	0	6036.96	−2.90	−2.13	−0.53	−2.47	3.24
0	0	3	6228.60	−0.39	0.67	−0.09	−0.13	−13.82
0	6	1	6254.38	−1.38	−0.42	−0.09	−1.89	−6.21
2	0	0	6519.61	−4.24	−3.29	−0.92	−0.51	6.13
1	2	1	6761.33	−2.57	−1.63	−0.46	1.35	−7.18
0	10	0	6855.53	−2.48	−1.06	−0.08	−1.28	−24.07
0	4	2	6951.68	−0.75	0.26	0.13	−1.60	−9.31
1	0	2	7455.42	−2.36	−1.14	−0.39	1.05	−6.17
0	2	3	7620.22	−1.17	−0.01	−0.59	1.02	2.98

^a“ad” refers to the adiabatic correction surface, “rel” to the relativistic one, and “NBO” to nonadiabatic corrections. Results are given in cm^{−1}; experimental levels (column “obs”) are from Mellau¹⁶ and Yang et al.²⁵ The results due to Varandas and Rodrigues⁴⁰ (Var. and Rod.) and Van Mourik et al.³ (VanMour.) are given for comparison.

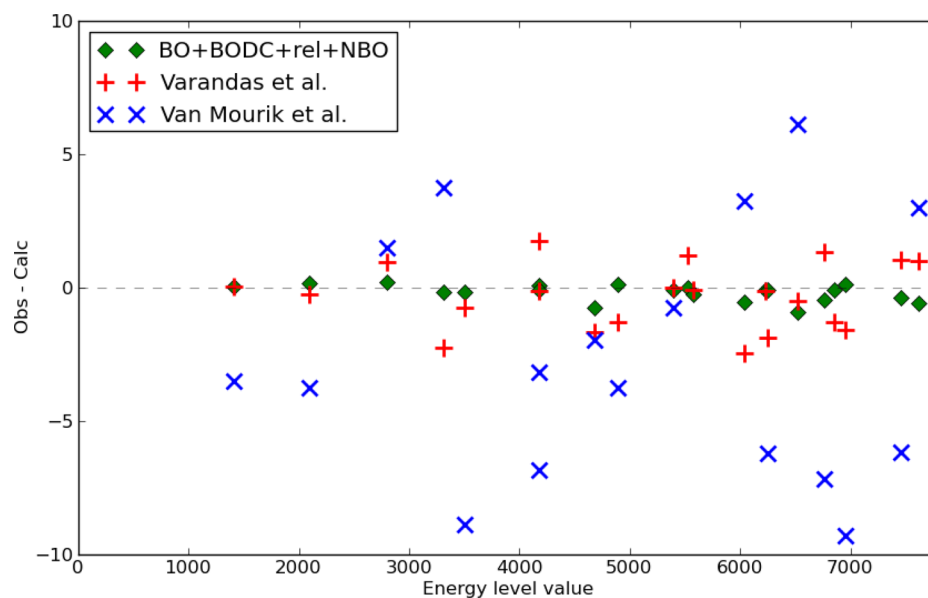


Figure 2. Differences of HCN vibrational levels compared to observation computed using the HCN-only PES (this work), by Varandas and Rodrigues,⁴⁰ and Van Mourik et al.³ (see Table 2). All values are in cm^{−1}.

determined to be $a = 1.42 \times 10^{-7}$ a.u. and $b = 1.94 \times 10^{-8}$ a.u. from the *ab initio* data.³⁷

This nonadiabatic correction was only tested in combination with the HCN-only PES (not the global HCN/HCN one); specifically, we looked at energy levels up to 7000 cm^{−1} for four HCN isotopologues.

4. RESULTS

The experimental energy levels which we use for comparison with our calculations are taken from the works of Mellau¹⁶ and

Yang et al.,²⁵ where almost all available vibrational levels up to 15 000 cm^{−1} are given, augmented by levels from Romanini and Lehmann²⁶ which span from 17 000 to 21 000 cm^{−1} for HCN stretching states only.

Table 2 compares our results obtained using the HCN-only PES with the previous *ab initio* calculations of Van Mourik et al.³ and with those by Varandas and Rodrigues,⁴⁰ who used an empirically determined PES. See also Figure 2 for a graphical illustration. It is particularly notable that for the HNC vibrational band origins we obtain a 10-fold improvement

Table 3. H¹²C¹⁴N Vibrational Band Origins in cm^{−1} up to 15 600 cm^{−1}, Calculated with the Global PES^a

ν_1	ν_2	ν_3	obs	obs – calc			
				BO	BO + ad + rel	Var. and Rod.	VanMour.
0	2	0	1411.42	0.06	0.18	0.03	−3.50
0	0	1	2096.85	0.32	0.67	−0.27	−3.73
0	4	0	2802.96	0.40	0.71	0.94	1.50
1	0	0	3311.48	−1.72	−1.25	−2.24	3.74
0	2	1	3502.12	−0.33	0.14	−0.77	−8.87
0	0	2	4173.07	0.38	1.09	0.22	−3.17
0	6	0	4174.61	−0.70	−0.08	1.42	−6.84
1	2	0	4684.31	−2.50	−1.93	−1.65	−1.97
0	4	1	4888.00	0.47	1.13	−1.30	−3.76
1	0	1	5393.70	−1.53	−0.68	0.01	−0.73
0	8	0	5525.81	−2.53	−1.54	1.19	−11.95
0	2	2	5571.89	−0.58	0.23	−0.07	−14.61
1	4	0	6036.96	−1.74	−0.97	−2.47	3.24
0	0	3	6228.60	0.28	1.34	−0.13	−13.82
0	6	1	6254.38	−0.33	0.63	−1.89	−6.21
2	0	0	6519.61	−3.53	−2.58	−0.51	6.13
1	2	1	6761.33	−2.18	−1.24	1.35	−7.18
0	10	0	6855.53	−4.30	−2.89	−1.28	−24.07
0	4	2	6951.68	0.57	1.58	−1.60	−9.31
1	0	2	7455.42	−1.71	−0.49	1.05	−6.17
0	2	3	7620.22	−1.08	0.09	1.02	2.98
2	2	0	7853.51	−5.28	−4.25	0.87	−2.32
1	4	1	8107.97	−1.53	−0.40	−1.86	−1.34
0	0	4	8263.12	−0.18	1.24	0.25	0.01
0	6	2	8313.53	1.03	2.33	0.17	0.25
2	0	1	8585.58	−3.51	−2.17	−2.36	−1.12
1	2	2	8816.00	−3.24	−1.93	−2.38	−1.96
0	4	3	8995.22	2.04	3.39	1.16	1.16
2	4	0	9166.62	0.83	−1.98	−4.90	−3.91
1	0	3	9496.44	−2.14	−0.54	−1.17	−0.58
3	0	0	9627.09	−4.71	−3.30	−3.89	−2.03
2	2	1	9914.40	−5.49	−4.07	−4.64	−3.85
2	0	2	10631.40	−3.89	−2.16	−2.65	−1.97
0	10	2	10974.20	−2.10	−0.75	−0.63	0.03
0	4	4	11015.90	−0.50	−0.78	1.07	1.20
1	0	4	11516.60	−2.66	−0.70	−1.71	−1.37
3	0	1	11674.50	−4.93	−3.13	−3.94	−3.09
0	6	4	12364.42	1.54	3.51	−0.72	−0.28
4	0	0	12635.89	−4.69	−2.84	−4.51	−2.66
2	0	3	12657.88	−4.47	−2.36	−3.35	−3.34
0	10	3	12999.49	−2.00	0.42	−1.39	−0.50
0	4	5	13014.80	2.20	4.23	0.60	0.92
0	2	6	13638.03	−1.35	0.86	−0.80	−0.85
3	0	2	13702.25	−5.45	−3.23	−1.40	2.82
0	6	5	14357.05	1.58	3.88	−1.78	−1.07
2	0	4	14653.66	−4.97	−2.63	3.90	−3.68
4	0	1	14670.45	−5.50	−3.14	−5.20	−5.62
3	2	2	14988.20	−3.66	1.10	−3.35	−2.76
0	4	6	14992.06	−4.12	−1.81	−4.37	−4.14
5	0	0	15551.94	−3.30	−1.11	−2.92	−1.32

^aSee the footnote of Table 2 to decipher the abbreviations. Results are given in cm^{−1}; experimental levels are from Mellau¹⁶ and Yang et al.²⁵ The results due to Van Mourik et al.,³ and Varandas and Rodrigues (Var. and Rod.)⁴⁰ are given for comparison.

compared to the previous *ab initio* calculations: 19 band origins up to 7 300 cm^{−1} are presented with a root-mean-square deviation $\sigma = 4.1$ cm^{−1}. In the more harmonic HCN system, which is easier to treat, we obtained $\sigma = 2.9$ cm^{−1} for the 50 observed vibrational energy levels below 15 600 cm^{−1}.

Using our calculated BODC and relativistic corrections, σ changes to 5.6 and 2.1 cm^{−1}, for HNC and HCN respectively. In addition, obtained $\sigma = 2.9$ cm^{−1} for the observed HCN vibrational levels in the 17 000 to 23 000 cm^{−1} region. Comparisons with previous, global PESs for HCN/HNC show an improvement of one or 2 orders of magnitude with

Table 4. Calculated $\text{H}^{12}\text{C}^{14}\text{N}$ Vibrational Band Origins, in cm^{-1} , above 15 600 cm^{-1} , Calculated Using the Global PES and Atomic Masses^{a,b}

ν_1	ν_2	ν_3	obs	BO		BO + ad + rel	
				calc	obs – calc	calc	obs – calc
5	0	1	17550.42	17554.61	–4.19	17552.07	–1.65
6	0	0	18377.03	18377.44	–0.41	18375.13	1.90
5	0	2	19528.58	19533.85	–5.27	19531.01	–2.43
6	0	1	20344.51	20346.25	–1.74	20343.68	0.83
7	0	0	21116.31	21112.75	3.56	21110.67	5.64
5	0	3	21486.77	21492.92	–6.15	21490.01	–3.24
6	0	2	22292.02	22295.35	–3.33	22292.50	–0.48
7	0	1	23047.11	23045.73	1.38	23043.59	3.52

^aThese levels were calculated with NPNT1 = NPNT2 = 60 and NALF = 90. ^bExperimental levels are from Romanini and Lehmann.²⁶

Table 5. Calculated $\text{H}^{14}\text{N}^{12}\text{C}$ Vibrational Band Origins in cm^{-1} , up to 15 600 cm^{-1} , Calculated Using the Global PES and Atomic Masses^a

ν_1	ν_2	ν_3	obs	BO		BO + BODC + rel		Var. and Rod.		Van Mourik et al.	
				calc	obs – calc	calc	obs – calc	calc	obs – calc	calc	obs – calc
0	2	0	926.50	926.48	0.02	925.69	0.82	926.48	0.02	941.92	–15.41
0	4	0	1867.06	1864.23	2.83	1862.45	4.61	1873.01	–5.95	1903.10	–36.04
0	0	1	2023.86	2023.69	0.17	2023.43	0.43	2023.65	0.21	2024.95	–1.09
0	6	0	2809.29	2802.76	6.53	2799.84	9.45	–	–	2834.81	–25.52
0	2	1	2934.82	2934.84	–0.02	2933.71	1.11	2934.70	0.12	2955.05	–20.23
1	0	0	3652.65	3657.39	–4.74	3656.43	–3.78	3651.84	0.81	3665.10	–12.45
0	8	0	3743.70	3736.81	6.89	3732.64	11.06	–	–	3759.86	–16.16
0	4	1	3861.43	3863.39	–1.96	3857.14	4.29	3868.36	–6.93	3902.41	–40.98
0	0	2	4026.49	4025.08	1.41	4024.53	1.96	4027.08	–0.59	4029.21	–2.72
1	2	0	4534.45	4539.22	–4.77	4537.34	–2.89	4536.00	–1.55	4558.15	–23.70
0	6	1	4790.86	4784.69	6.17	4781.28	9.58	–	–	4820.95	–30.09
0	2	2	4921.24	4923.83	–2.59	4919.04	2.20	–	–	4946.74	–25.50
1	4	0	5428.98	5430.09	–1.11	5427.15	1.83	5435.81	–6.83	5469.23	–40.25
1	0	1	5664.85	5668.46	–3.61	5667.21	–2.36	5664.55	0.30	5676.51	–11.66
0	4	2	5833.43	5828.75	4.68	5826.12	7.31	–	–	5879.59	–46.16
1	6	0	6322.72	6318.88	3.84	6314.72	8.00	–	–	6354.07	–31.35
1	2	1	6532.40	6535.74	–3.34	6533.52	–1.12	–	–	6558.72	–26.32
2	0	0	7171.41	7178.70	–7.29	7171.99	–0.58	7171.33	0.08	7189.47	–18.06
1	8	0	7205.16	7201.62	3.54	7196.10	9.06	–	–	7226.47	–21.31

^aExperimental levels are from Mellau.²³ The results due to Van Mourik et al.,³ and Varandas and Rodrigues (Var. & Rod.)⁴⁰ are given for comparison.

previous *ab initio* results and comparable accuracy with the fitted PES of Varandas and Rodrigues⁴⁰ for low-lying energies and an order of magnitude improvement for energies lying between 10 000 and 14 000 cm^{-1} .

The second column of Table 2 gives the results including the relativistic and BODC correction surfaces. These results are of a quality similar to those in column 1 of Table 1 of our study on water,⁷⁵ which demonstrates the similarity between the two calculations. This is an important point as it suggests the high accuracy results obtained for water can indeed be extended to systems with more than one second-row atom and more electrons; this is one of the goals of this paper.

The results of our global calculations of both HCN and HNC levels up to the energies of 25 000 cm^{-1} are presented in Tables 3, 4 and 5. Below the barrier to isomerization the density of states is quite low and matching observed and calculated energy levels is unequivocal; for higher energy levels we had to employ additional procedures to confirm the quantum number assignment of the calculated energy levels when compared with the experimental ones. It could be seen

from Table 4 that excellent *ab initio* accuracy for these highly excited energy levels is achieved for the first time.

We used three methods to determine the value of ν_2 for the calculated levels. The first method involved the calculation of the diagonal matrix elements $\langle \psi_i | X_{\text{bend}}^2 | \psi_i \rangle$, where X_{bend} is the bending coordinate, by numerical integration of the corresponding wave functions.⁷⁰ The second method monitored the sensitivity of the calculated energy to small bending-angle-dependent changes to the potential. These two independent methods both distinguish between high ν_2 and low ν_2 levels. They helped to confirm that our matches of the experimentally determined and calculated energy levels to levels with $\nu_2 = 0$ are correct. The third method consists in counting nodes in wave functions. The higher the energy of HCN, the closer pure stretching energy levels to each other, and the previously described labeling methods become insufficient. For example, the state (8 0 0) has energy $E = 23\,766\text{ cm}^{-1}$ and state (0 0 12) has $E = 23\,779\text{ cm}^{-1}$; i.e., they are only 13 cm^{-1} away from each other. On the other hand, the density of states is approximately 11 $\text{cm}^{-1}/\text{state}$ at these energies. We therefore resorted to plotting the corresponding wave functions to assign the

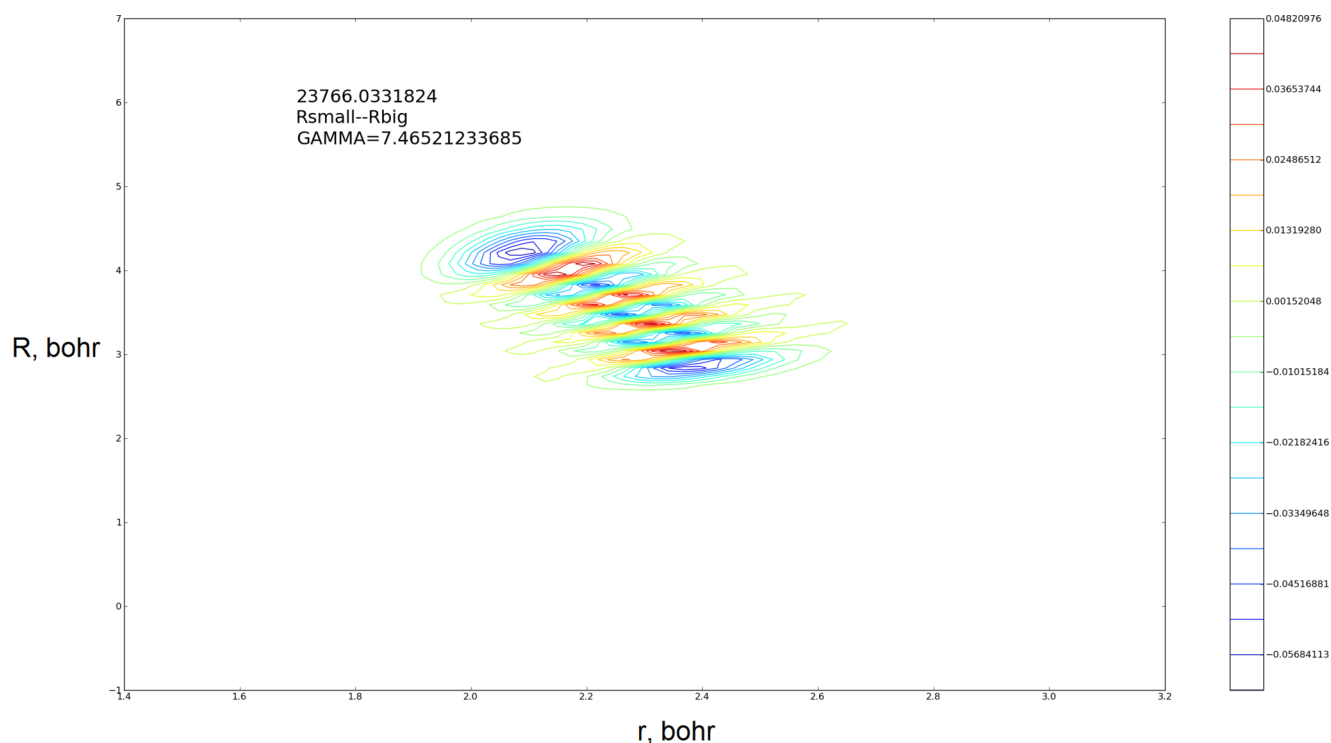


Figure 3. (8 0 0) state, $\psi = \psi(R;r)|\gamma = 7.4652$ degree cut.

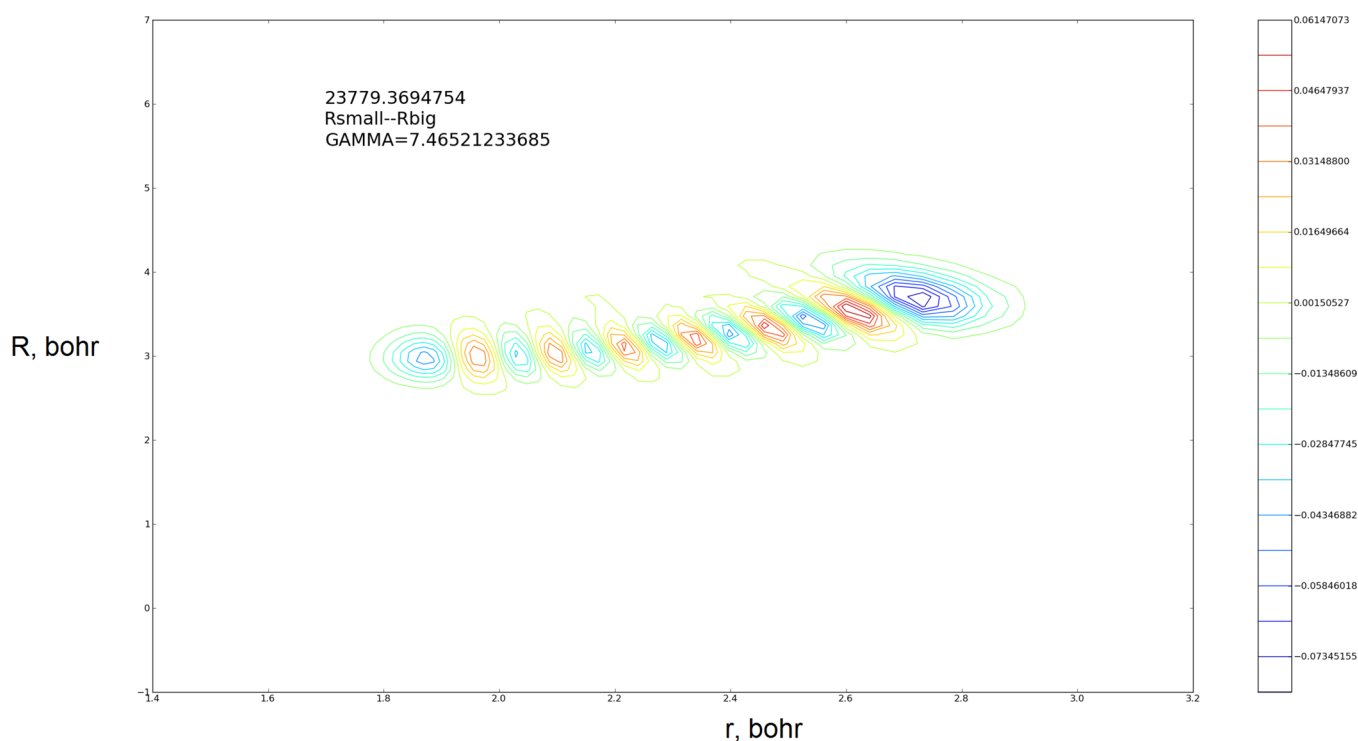


Figure 4. (0 0 12) state, $\psi = \psi(R;r)|\gamma = 7.4652$ degree cut.

quantum numbers in these cases; see Figures 3 and 4. Plotting of wave functions was also used to verify the assignment of all vibrational levels (see Table 6).

Results of calculations on HNC (the second well) are given in Table 5. As for HCN, a significant improvement on the results of Van Mourik et al.³ can be seen.

Table 6 presents the calculations of all energy levels up to 10 000 cm^{-1} with quantum numbers assignment to all (except

one) calculated energy levels; the corresponding experimental energy levels are also given where available. A table of term values for rotationally excited levels $J \leq 9$ is given in the Supporting Information. Note that vibrational levels with $l=0$ can only be calculated for $J=0$ because of the linearity of the molecule. The other lowest bending states, such as $\nu_1\nu_2^l\nu_3=0$ $1^10, 0\ 3^10, 0\ 3^30, \dots, 0\ 9^10, 0\ 9^30, 0\ 9^50, \dots, 0\ 9^90$, only occur

Table 6. Assigned Vibrational Levels of $\text{H}^{12}\text{C}^{14}\text{N}$ with $l = 0$ below $10\,000\text{ cm}^{-1}$ Calculated Using the HCN-Only PES^a

state			obs	calc
ν_1	ν_2	ν_3		
0	2	0	1411.42	1411.37
0	0	1	2096.85	2096.70
0	4	0	2802.96	2802.76
1	0	0	3311.48	3311.66
0	2	1	3502.12	3502.30
0	0	2	4173.07	4172.97
0	6	0	4174.61	4174.71
1	2	0	4684.31	4685.04
0	4	1	4888.00	4887.88
1	0	1	5393.70	5327.67
0	8	0	5525.81	5525.80
0	2	2	5571.89	5572.15
1	4	0	6036.96	6037.49
0	0	3	6228.60	6228.69
0	6	1	6254.38	6254.47
2	0	0	6519.61	6520.53
1	2	1	6761.33	6761.79
0	10	0	6855.53	6855.61
0	4	2	6951.68	6951.55
1	6	0	—	7370.75
1	0	2	7455.42	7455.81
0	8	1	—	7600.73
0	2	3	7620.22	7620.81
2	2	0	7853.51	7856.01
1	4	1	8107.97	8108.61
0	12	0	—	8163.03
0	0	4	8263.12	8263.74
0	6	2	8313.53	8312.62
2	0	1	8585.58	8586.57
1	8	0	—	8683.04
1	2	2	8816.00	8817.59
1	10	0	—	8925.44
0	4	3	8995.22	8993.73
2	4	0	9166.62	9169.40
1	6	1	—	9436.62
0	14	0	—	9444.77
1	0	3	9496.44	9497.39
3	0	0	9627.09	9628.75
0	2	4	—	9648.20
0	8	2	—	9653.87
2	2	1	9914.40	9917.34
1	10	0	—	9973.45

^aResults are given in cm^{-1} ; experimental levels are from Mellau¹⁶ and Yang et al.²⁵

for $J = l$. For all the 70 band origins with both $J = 0$ and excited J the root-mean-square deviation σ from the experimental levels reached 0.3 cm^{-1} . For 122 known levels of $J = 9$ we have $\sigma = 0.39\text{ cm}^{-1}$. Thus, both vibrational and rotational levels of HCN and isotopologues have been calculated with a standard deviation of around 0.3 cm^{-1} .

We use our HCN-only PES and our mass-dependent adiabatic surface to predict the energy levels of three minor isotopologues: $\text{H}^{13}\text{C}^{14}\text{N}$, $\text{H}^{12}\text{C}^{15}\text{N}$ and $\text{D}^{12}\text{C}^{14}\text{N}$. The accuracy of HCN levels below 7800 cm^{-1} is improved to 1.2 cm^{-1} with these *ab initio* calculations (Table 2, column “+ad + rel”). Using empirically determined NBO correction, σ changes to 0.37 cm^{-1} (column “+NBO”). Initially we determined the non-

adiabatic correction constants a and b uniquely from the $\text{H}^{12}\text{C}^{14}\text{N}$ major isotopologue. However, we found that in this case the difference between the calculated and experimental levels for the DCN isotopologue were sometimes even worse than without nonadiabatic corrections. We therefore repeated the optimizations considering both the HCN and DCN isotopologues. Finally we were able to reproduce the HCN vibrational energy levels below 7000 cm^{-1} for all four isotopologues with $\sigma = 0.37\text{ cm}^{-1}$. Results for DCN are summarized in Table 7 and also give $\sigma = 0.37\text{ cm}^{-1}$. Results for $\text{H}^{13}\text{C}^{14}\text{N}$ are summarized in Table 8 and give $\sigma = 0.38\text{ cm}^{-1}$. Results for $\text{H}^{12}\text{C}^{15}\text{N}$ are summarized in Table 9 and give $\sigma = 0.36\text{ cm}^{-1}$.

Dissociation Energy. The dissociation energy D_0 of a molecule is a standard thermochemical parameter and in the case of HCN corresponds to the reaction $\text{HCN}(\tilde{X}^1\Sigma) \rightarrow \text{H}(^2S) + \text{CN}(\tilde{X}^2\Sigma^+)$; in the usual Born–Oppenheimer (or adiabatic) approximation the dissociation energy D_0 is related to the potential well depth D_e by

$$D_0 = D_e + \text{ZPE}(\text{CN}) - \text{ZPE}(\text{HCN}) \quad (10)$$

where the zero-point energy (ZPE) is defined here as the energetic difference between the bottom of the potential well and the energy of the ground rotation–vibrational ground state. The potential well depth D_e is defined by

$$D_e = E_{\text{H}} + E_{\text{CN}} - E_{\text{HCN}} \quad (11)$$

where the electronic energies for CN and HCN are computed with the nuclei fixed at their equilibrium positions.

Although very accurate spectroscopic measurements of D_0 of the type of ref 77 have not been performed for HCN, several values have been reported in the literature. The three most recent and accurate experiments are $43\,740 \pm 150\text{ cm}^{-1}$ by Morley et al.,⁷⁸ $43\,710 \pm 70\text{ cm}^{-1}$ by Cook et al.,⁷⁹ and $43\,715 \pm 32\text{ cm}^{-1}$ by Hu et al.¹⁰ These values are clustered close together and differ by much less than their uncertainties.

We computed D_e both using the same level of MRCI theory used for the construction of the PES produced in this work as well as using coupled cluster theory. In the MRCI calculation the HCN potential well depth was computed as the difference in energy between HCN at the equilibrium geometry ($r_{\text{CH}} = 2.0125\text{ a}_0$, $r_{\text{CN}} = 2.1793\text{ a}_0$) and HCN with the CH bond highly stretched and the CN bond relaxed to the CN diatomic equilibrium bond length ($r_{\text{CH}} = 20\text{ a}_0$, $r_{\text{CN}} = 2.2144\text{ a}_0$). Analysis for $r_{\text{CH}} > 13\text{ a}_0$ shows that the HCN potential behaves as $D_e - (c/r_{\text{CH}})^6$ where $c = 9.81\text{ a}_0\text{ cm}^{-1/6}$, so that our chosen stretched geometry with $r_{\text{CH}} = 20\text{ a}_0$ differs from D_e by less than 0.02 cm^{-1} . In the coupled cluster calculations D_e was obtained as the difference between the energy of HCN at equilibrium and the sum of the energies of the open-shell CN diatomic at equilibrium and one hydrogen atom. The calculations used Molpro and MRCC.^{80,81} Coupled cluster calculations are expected to be very accurate as only calculations at equilibrium are needed and the coupled cluster hierarchy is known to converge very quickly in this situation. Our results are summarized in Table 11, which is described in detail in the next section.

Calculation Details. Line A is the basis set extrapolation carried out using formula 2, namely $E_{\text{ac}[56]z} = E_6 + 1.051795977(E_6 - E_5)$. The uncertainty was taken as one-half of the difference between the ac6z and the ac[56]z extrapolated value. The acS_z and ac6z values are, respectively, $46\,327$ and $46\,368\text{ cm}^{-1}$. All electrons were correlated. All coupled cluster

Table 7. D¹²C¹⁴N Vibrational Band Origins in cm^{−1} Computed with the HCN-Only PES^a

ν_1	ν_2	ν_3	obs	BO		BO + BODC + rel		BO + BODC + rel + NBO	
				calc	obs − calc	calc	obs − calc	calc	obs − calc
0	2	0	1129.99	1130.33	−0.34	1130.35	−0.36	1129.96	0.03
0	0	1	1925.26	1925.85	−0.59	1925.53	−0.27	1924.78	0.48
0	4	0	2243.96	2244.40	−0.44	2244.41	−0.45	2243.65	0.31
1	0	0	2630.30	2631.64	−1.34	2631.47	−1.17	2630.12	0.18
0	2	1	3060.68	3061.81	−1.13	3061.50	−0.82	3060.38	0.30
0	6	0	3342.56	3343.59	−1.03	3343.54	−0.98	3342.40	0.16
0	0	2	3729.13	3731.23	−2.10	3731.09	−1.96	3729.38	−0.25
1	2	0	3836.35	3837.94	−1.59	3837.28	−0.93	3835.80	0.55
0	8	0	4426.17	4427.85	−1.68	4427.67	−1.5	4426.16	0.01
0	2	2	4523.28	4525.35	−2.07	4524.85	−1.58	4522.76	0.52
2	0	0	5220.22	5222.85	−2.62	5222.50	−2.28	5219.89	0.33
0	10	0	5494.94	5497.00	−2.06	5496.66	−1.72	5494.79	0.15
1	0	2	6401.58	6404.69	−3.11	6403.85	−2.27	6401.02	0.56
2	0	1	7080.10	7083.76	−3.66	7083.08	−2.98	7079.73	0.37
3	0	0	7771.47	7775.35	−3.88	7774.82	−3.35	7771.02	0.45
2	0	2	8924.68	8929.52	−4.84	8928.50	−3.82	8924.42	0.26

^aExperimental levels were taken from from Carter et al.⁷⁶Table 8. H¹³C¹⁴N Vibrational Band Origins in cm^{−1} Computed with the HCN-Only PES^a

ν_1	ν_2	ν_3	obs	BO		BO + BODC + rel		BO + BODC + rel + NBO	
				calc	obs − calc	calc	obs − calc	calc	obs − calc
0	2	0	1399.76	1400.42	−0.66	1400.43	−0.67	1399.88	−0.12
0	0	1	2063.05	2063.54	−0.49	2063.18	−0.13	2062.88	0.16
0	4	0	2780.59	2781.86	−1.28	2781.82	−1.24	2780.72	−0.14
1	0	0	3293.51	3296.28	−2.77	3296.09	−2.57	3293.87	−0.36
0	2	1	3455.79	3457.30	−1.51	3456.95	−1.16	3456.11	−0.32
0	0	2	4105.87	4107.03	−1.15	4106.30	−0.42	4105.72	0.16
0	6	0	4142.36	4144.80	−2.44	4144.61	−2.25	4142.98	−0.62
1	2	0	4655.84	4659.78	−3.94	4659.62	−3.78	4656.89	−1.05
0	4	1	4830.25	4832.19	−1.93	4831.78	−1.53	4830.40	−0.15
1	0	1	5343.66	5347.00	−3.35	5346.43	−2.77	5343.92	−0.26
0	8	0	5484.47	5487.71	−3.25	5487.31	−2.84	5485.16	−0.69
2	0	0	6483.28	6489.24	−5.96	6488.83	−5.55	6484.57	−1.29
1	2	1	6699.10	6704.03	−4.93	6703.49	−4.39	6700.48	−1.38
0	10	0	6805.80	6810.10	−4.29	6809.45	−3.64	6806.78	−0.98
2	2	0	7807.96	7816.07	−8.10	7815.70	−7.73	7810.95	−2.99
1	4	1	8035.77	8040.97	−5.19	8040.36	−4.59	8036.86	−1.09
2	0	1	8519.24	8525.92	−6.68	8525.12	−5.88	8520.55	−1.31
2	4	0	9113.10	9121.76	−8.66	9121.32	−8.22	9116.10	−3.00
3	0	0	9571.70	9580.68	−8.98	9580.05	−8.35	9573.91	−2.21
2	2	1	9837.71	9846.90	−9.19	9846.14	−8.43	9841.10	−3.39
2	6	0	10398.58	10409.36	−10.77	10408.74	−10.15	10403.05	−4.47
3	2	0	10858.19	10870.46	−12.27	10869.85	−11.66	10863.26	−5.07

^aExperimentental levels are from Hofmann et al.²⁴ and Maki et al.¹⁴

calculations were performed on a single core of a 3.4 GHz i7–3770 workstation and the CCSD(T)/ac6z calculation for HCN took about 4.2 h. Note that the value reported was obtained using the spin-unrestricted RHF-UCCSD(T) variant of coupled cluster for the CN diatomic; the consequences of this choice are discussed in the following section. Line B, the CCSDTQ-CCSD(T) correction, is -219 cm^{-1} in the 2z basis set and -226 cm^{-1} in the 6-31G basis set. The assigned overall uncertainty includes the difference of the 2z and 6-31G values multiplied by an (arbitrary and hopefully conservative) factor 2 to allow for the lack of core correlation in the correction and for further basis set dependence. The CCSDTQ/3z took 8.6 h. Line C: The CCSDTQP-CCSDTQ correction is -21 cm^{-1} in

the 6-31G basis set and -11 cm^{-1} in the cc-pVDZ one; the given uncertainty is the difference between the 2z and 6-31G values. We also computed a FCI-CCSDTQP correction in the 6-31G basis set and it came out -2 cm^{-1} . In view of its smallness it was neglected. The CCSDTQP/2z calculation took 3.0 h. Line E: MRCI calculations used the 10-electron, 10-orbital CAS described in the text (also used to compute both our PESs) comprising 8 orbitals of a' symmetry and 2 orbitals of a'' symmetry; the basis set extrapolation and its relative uncertainty were calculated as described in [ab initio calculation](#) section above. The reported uncertainties only account for basis set uncertainty but not incomplete correlation treatment. Line F is the MRCI including Davidson correction using the fixed-

Table 9. H¹²C¹⁵N Vibrational Band Origins in cm^{−1} Computed with the HCN-Only PES^a

ν_1	ν_2	ν_3	obs	BO		BO + BODC + rel		BO + BODC + rel + NBO	
				calc	obs − calc	calc	obs − calc	calc	obs − calc
0	2	0	1409.31	1409.96	−0.66	1409.83	−0.53	1409.24	0.07
0	0	1	2064.32	2064.82	−0.50	2064.48	−0.16	2064.16	0.15
0	4	0	2798.64	2799.92	−1.28	2799.58	−0.94	2798.40	0.23
1	0	0	3310.09	3312.86	−2.77	3312.38	−2.29	3310.22	−0.13
0	2	1	3467.78	3469.30	−1.51	3468.82	−1.04	3467.93	−0.15
0	0	2	4108.64	4109.82	−1.18	4109.13	−0.49	4108.52	0.12
0	6	0	4167.99	4170.43	−2.44	4169.79	−1.80	4168.04	−0.05
0	4	1	4851.83	4853.78	−1.95	4853.11	−1.27	4851.64	0.20
1	0	1	5360.25	5363.61	−3.35	5362.77	−2.52	5360.29	−0.04
0	8	0	5516.84	5520.09	−3.25	5519.07	−2.23	5516.77	0.07
2	0	0	6725.25	6730.20	−4.95	6729.25	−4.01	6726.24	−0.99

^aExperimental levels are from Maki et al.¹⁴

reference coefficient (as used for the global PES). The Davidson value using relaxed reference is 43 795 cm^{−1}, while the Pople corrected value with fixed/relaxed references are 43 715 and 43 762 cm^{−1}. The reported uncertainty comes from combining the uncertainty due to basis set extrapolation, 20 cm^{−1}, and the standard deviation of the four MRCI corrected values, 33 cm^{−1}, taken as an estimate of the error in correlation treatment. Line G: Relativistic corrections computed either with MRCI/ac6z and the MVD1 Hamiltonian or using CCSD(T)/acSz-DK and the Douglas–Kroll–Hess Hamiltonian give −22 cm^{−1} with a scatter of about 1 cm^{−1}. Line H: Adiabatic correction based on CCSD wavefunction computed using an aug-cc-pVTZ basis set gives about +11 cm^{−1}. Line I is the value obtained using our final HCN PES and the DVR3D software suite. The assigned uncertainty of 1.5 cm^{−1} reflects the scatter due to using atomic or nuclear masses and on whether the nonadiabatic corrections are included or not. Line J: The zero-point energy for the CN diatomic was computed using the constants reported by Irikura⁸² and his formulas (4) and (5); the original values for the constants come from ref 83. Note that the formulas (4) and (5) used assume an isolated ¹Σ ground state with a rotational $J = 0$ ground state; in the case of CN, its ²Σ ground state has $J = 1/2$ and so use of those formulas leads to a ZPE which is too small by about 1.4 cm^{−1}. Nevertheless, we ignore this small contribution as it is much smaller than other sources of uncertainty.

Dependence on the Choice of the Open-Shell Coupled Cluster Variant. There are many variants of coupled cluster methods for open-shell systems.^{84,85} The UCCSD(T) method implemented in Molpro⁸⁴ is a particular variant based on a spin-restricted open-shell Hartree–Fock reference although spin contamination is introduced by the method. In fact ref⁸⁴ reports (as its Figure 1) a plot of $S^2 - S(S + 1)$ from which one can see that near equilibrium ($r \approx 2.2$ a₀) the quoted quantity is ≈ 0.012 instead of zero. Molpro also implements also another, partially spin-restricted variant, RCCSD(T). There is no reason to expect one variant to be more accurate than the other and they are found to give similar results in terms of computed properties such as equilibrium bond lengths, vibrational frequencies.⁸⁴ For the CN ground state at equilibrium ($r = 2.2144$ a₀) the UCCSD(T) variant gives absolute energies which are lower than the one given by RUCCSD(T), as shown in the Table 10: As it can be seen from Table 10, the limit value for large basis sets of the RCCSD(T) – UCCSD(T) absolute energy difference for CN at equilibrium is 241 cm^{−1}, a value which might look worrying large; however, because we

Table 10. *Ab Initio* Coupled Cluster Energies for the CN Diatomic at Equilibrium ($r = 2.2144$ a₀) for Two Variants of the CCSD(T) Method^a

basis set	frozen core	E_h		diff. (cm ^{−1})
		RCCSD(T)	UCCSD(T)	
cc-pVDZ	yes	−92.489850	−92.490609	167
cc-pVTZ	yes	−92.566508	−92.567490	216
cc-pCVTZ	no	−92.671262	−92.672307	229
aug-cc-pCVQZ	no	−92.704429	−92.705517	239
aug-cc-pCVSZ	no	−92.712836	−92.713929	240
aug-cc-pCV6Z	no	−92.715873	−92.716968	240
aug-cc-pCV[56]Z	no	−92.719067	−92.720163	241

^aThe column labelled “diff.” reports RCCSD(T) – UCCSD(T).

supplement the UCCSD(T) energies with high-order coupled cluster corrections (up to CCSDTQP), the actual dependence of our final value of D_0 (line L in Table 11) on the choice of the CCSD(T) open-shell variant is much smaller, only about 25 cm^{−1}. To be explicit, the nonrelativistic part of the electronic

Table 11. *Ab Initio* Contributions to the Dissociation Energies of HCN^a

label	description	value	error
A	CCSD(T)/ac[56]z	46411	(22)
B	CCSDTQ/3z	−217	(35)
C	CCSDTQP/2z	−11	(10)
D	best coupled-cluster D_e [=A + B + C]	46183	(41)
E	MRCI/ac[56]z	45936	(20)
F	MRCI+Q-f/ac[56]z	46209	(39)
G	relativistic correction	−22	(1)
H	adiabatic correction (BODC)	+11	
I	zero point energy HCN	3474	(1.5)
J	zero point energy CN	1031	(1)
K	overall zero point energy contribution [=I − J]	−2443	(2)
L	best coupled cluster D_0 [=D + G + H + K]	43729	(35)
M	best MRCI D_0 [=E + G + H + K]	43755	(30)
N	experimental D_0 from ref 10	43715	(32)
O	experiment–theory/coupled cluster [=N − L]	−14	(44)
P	experiment–theory/MRCI [=N − M]	−40	(50)

^aAll values are in cm^{−1}. Bolded contributions are additive corrections. Quantities A to H are nuclear-mass independent; all others are nuclear-mass dependent. See text for a full description of the contributions.

energy $E(\text{CN})$ appearing in eq 11 and contributing to line D in Table 10 is given by

$$E^{(U)} = E_{\text{UCCSD(T)}}^{ac[56]z} + (E_{\text{CCSDTQ}}^{3z} - E_{\text{UCCSD(T)}}^{3z}) + (E_{\text{CCSDTQP}}^{2z} - E_{\text{CCSDTQ}}^{2z}) \quad (12)$$

This formula, which is in the spirit of extrapolation schemes such as HEAT⁴³ or the focal-point analysis,⁴⁴ is based on the assumption that error due to basis set incompleteness and the one due to incomplete electron correlation are approximately independent. In the formula above the CCSDTQ and CCSDTQP calculations were made with MRCC,^{80,81} which uses spin-unrestricted variants for open-shells. Note that both spin-unrestricted spin-restricted variants of the coupled cluster hierarchy will converge to the same, FCI, value as higher and higher excitations are included. Had we used the RCCSD(T) variant for the large basis calculations, we would have obtained an energy $E^{(R)}$ given by

$$E^{(R)} = E_{\text{RCCSD(T)}}^{ac[56]z} + (E_{\text{CCSDTQ}}^{3z} - E_{\text{RCCSD(T)}}^{3z}) + (E_{\text{CCSDTQP}}^{2z} - E_{\text{CCSDTQ}}^{2z}) \quad (13)$$

The difference $E^{(R)} - E^{(R)}$ (and the corresponding shift in the HCN D_e) amounts therefore to

$$E^{(R)}(\text{CN}) - E^{(R)}(\text{CN}) = (E_{\text{RCCSD(T)}}^{ac[56]z} - E_{\text{UCCSD(T)}}^{ac[56]z}) - (E_{\text{RCCSD(T)}}^{3z} - E_{\text{UCCSD(T)}}^{3z}) \quad (14)$$

If the basis set and electron correlation errors were exactly independent, this difference would evidently be zero. In actual practice from the value reported in Table 10, one can see that the expression above amounts to 25 cm⁻¹. This value was used as a contribution to the overall uncertainty bundle of the CCSDTQ correction in Table 11. The situation could be improved by performing the CCSDTQ correction in a larger basis set: e.g., the shift given by expression 14 would be reduced to 11 cm⁻¹ using the cc-pCVTZ basis set and doing all-electron calculations.

Comments. The results in Table 11 show that our theoretical values, both using coupled cluster and MRCI+Q, agree well with one another as well as with the best experimental value. Our theoretical results suggest that the experimental value $D_0 = 43\,715(32)$ cm⁻¹ may be too small by 10–20 cm⁻¹, although the evidence for this is weak.

Our MRCI+Q (fixed reference) value agrees to 25 cm⁻¹ with the highly accurate high-order coupled cluster, which should be considered an extremely good result and indicates that our PES should be of high accuracy also in the high energy region. Of notice is the MRCI+Pople (fixed reference) value, which agrees with the coupled cluster to within only 3 cm⁻¹, although this is just a fortuitous coincidence.

Isomerization Energy. We now consider the difference in energy between the lowest rotational–vibrational states of HCN and of HNC (Figure 5). Van Mourik et al.³ computed this difference to 5180 cm⁻¹. However, Barber et al.⁶ chose to use a value of 5720 cm⁻¹, which was criticized as being too high by Nguyen et al.⁵ Nguyen et al. calculated a value of 5236 cm⁻¹ using CCSDTPQ together with BODC and relativistic corrections. Nguyen et al. also give the isomerization energy as determined by the active thermochemical tables (ATcT) (this approach is described by Ruscic et al.⁸⁶). The ATcT result

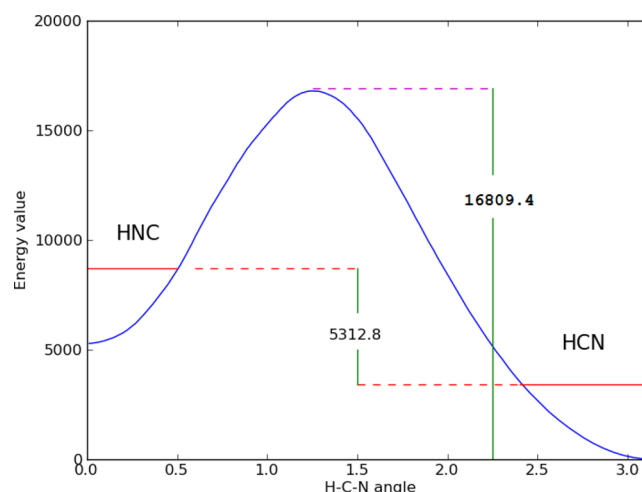


Figure 5. Lowest-energy isomerization path (in blue) and ground vibrational states (in red) of HCN and HNC depends on θ (see eq 7). Angle is in radians, energy values are in cm⁻¹.

is 5212 cm⁻¹, which is lower than the calculated value of Nguyen et al. by 24 cm⁻¹. However, this result used $\Delta E_{\text{ZPE}} = -88$ cm⁻¹ for the zero point energy correction and this value does not agree well with our present calculations performed using a very accurate PES and variational nuclear motion calculations. We note that the HNC bending motion is particularly anharmonic and requires a full treatment if accurate results are to be obtained. Our calculations give a ΔE_{ZPE} in the range -99 to -109 cm⁻¹ depending on the size extensivity correction used for the PES (see Table 12); specifically, we obtain $\Delta E_{\text{ZPE}} = -108.5$ cm⁻¹ for Pople “fixed reference” size extensivity, which we used for our HCN-only PES. If we substitute 88 cm⁻¹ of Nguyen et al. value of ΔE_{ZPE} , the resulting isomerization energy, 5 216 cm⁻¹, agrees almost perfectly with ATcT value. As one can see from the Table 12 the results of the isomerization energy calculation have some dependence on the size extensivity choice, with the maximum difference between different size extensivity corrections being about 60 cm⁻¹. This value can be taken as an estimate of the uncertainty of the computed values. Our Davidson “fixed reference” results differ by about 70 cm⁻¹ from Nguyen et al. (corrected results) as well as from ATcT, and this discrepancy is compatible with the uncertainty estimate mentioned above.

Table 13 shows how the different size extensivity corrections affect at the height of the barrier to isomerization ($\Delta E_{\text{barrier}}$). We can estimate the calculation error caused by the choice of size extensivity correction by comparing them; the value of this error is about 25 cm⁻¹. This suggests our value of the barrier height is 16 809.4 cm⁻¹. This value agrees well with the previous *ab initio* calculations by van Mourik et al.³ but is somewhat higher than the one from the observations by Baraban et al.¹ This disagreement may be caused by the geometry used for the saddle point. In our case we found the saddle point to be located at $(r_{\text{CH}}, r_{\text{CN}}, \theta) = (2.238\,a_0, 2.242\,a_0, 71.29^\circ)$ by surface extremum search (see Figure 6).

5. DISCUSSION

The new *ab initio* PESs presented here improve the accuracy of previous *ab initio* calculations of HCN rotational–vibrational energy levels by more than 10 times, and it is hoped that they will help solving some of the existing issues in HCN spectroscopy. A global line list of HCN/HNC transitions

Table 12. Energy Difference, ΔE in cm^{-1} , between the Lowest Levels of HCN and HNC as a Function of the Size Extensivity Correction Employed^a and Compared to the Values of Nguyen et al.⁵

size extens.	+Q fix.	+Q rel.	+P fix.	+P rel.	Nguyen et al.	ATcT
ΔE_{BO}	5388.1	5413.7	5416.3	5440.2	5321	—
ΔE_{BODC}		−6.4			−7	—
ΔE_{rel}		+11.4			12	—
ΔE_{ZPE}	−109.1	−98.7	−108.5	−100.3	−88	—
$\Delta E_{\text{HNC}}^0 - E_{\text{HCN}}^0$	5284.0	5320.0	5312.8	5344.9	5236	5212

^a+Q indicates the renormalised Davidson correction, +P the Pople correction and fix./rel. whether the fixed-reference or relaxed-reference values were used.

Table 13. Height of HCN–HNC Barrier in cm^{-1} as a Function of the Size Extensivity Correction (See Table 12 for Deciphering the Acronyms)

size extens.	+Q fix.	+Q rel.	+P fix.	+P rel.	Van Mourik et al. ³	Baraban et al. ¹
ΔE_{BO}	16792.1	16777.7	16821.2	16808.1	16814	—
ΔE_{BODC}		+7.3			+8	—
ΔE_{rel}		−19.1			−24	—
$\Delta E_{\text{barrier}}$	16780.3	16765.9	16809.4	16796.3	16798	16695(17)

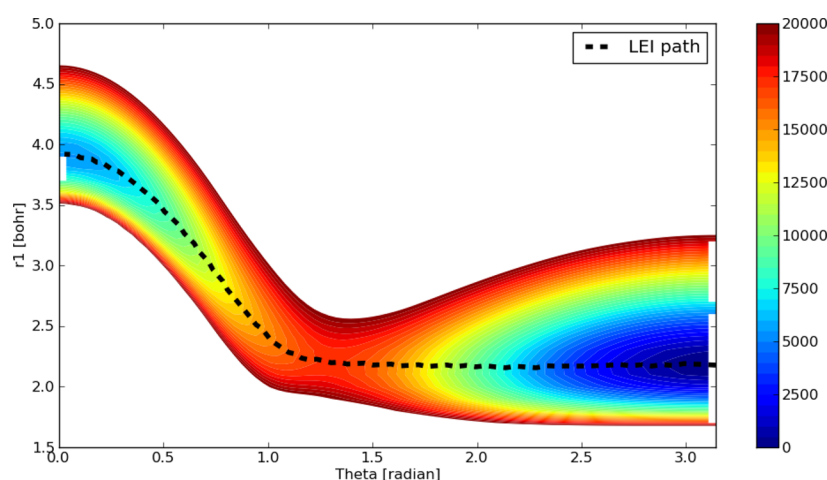


Figure 6. Potential energy surface, in cm^{-1} , showing the lowest-energy isomerization (LEI) path between HCN and HNC for a C–N bond length fixed at $2.2 a_0$.

calculated using our new PES should give a significantly improved representation of the combined HCN/HNC spectrum, and could be used for applications to astrophysics and studies of planetary atmospheres. The estimated accuracy of $\pm 40 \text{ cm}^{-1}$ in the dissociation energy suggests that a similar accuracy could be achieved for HCN/HNC rovibrational levels up to dissociation using the same *ab initio* methodology. The extension to a HCN/HNC global surface will be the subject of future work.

The *ab initio* accuracy of energy levels up to $10\,000 \text{ cm}^{-1}$ is of particular note, as it is more accurate on average than the accuracy of the PES by Varandas and Rodrigues,⁴⁰ which was fitted to experimental energy levels.

The accuracy of our *ab initio* treatment of the HCN molecule is worse than the 0.1 cm^{-1} level of accuracy achieved for water.³⁷ We believe that the major reason for this is a insufficient level of electron correlation treatment at the MRCI level. Nevertheless our results suggest that near-experimental accuracy we achieved in *ab initio* calculations on water³⁷ could be successfully achieved for molecules with two second-row atoms and containing more electrons than water. A significant improvement in *ab initio* calculations for similar molecules, such as C_2H_2 , the $(\text{HF})_2$ dimer and others should be possible

using methods employed in the present calculations. This will be a subject of future studies.

We determine the isomerization energy to be 5312 cm^{-1} from Pople “fixed reference” calculations (the same level of theory used for our global PES). A somewhat lower value of 5284 cm^{-1} was determined using Davidson “fixed reference” size extensivity corrections. This value agrees with ATcT at 5212 cm^{-1} and Nguyen et al. at 5236 cm^{-1} within the estimated error of our calculations.

Accurate determination of the energy around the saddle point is of particular interest. Recent investigations of a new type of vibrational wave functions around the saddle point² shows the necessity of a better theoretical description of the effects around transition states (see also ref 1). The experimental estimation of the barrier height in ref 1 differs from the previous *ab initio* calculations by a significant amount, about 100 cm^{-1} .

Our global PES is a suitable tool for the calculations of the energy levels up to dissociation and in principle (provided such experimental data do exist) could be used for possible assignment of double and triple resonance lines similar to what we have done for water.^{87–90} However, it should be noted that while our final PES describes well the HCN and HCN

vibrational energy levels, the isomerization dynamics are probably not described with same level of accuracy.

Additional information related to the choice of the CAS and the size-extensivity correction, as well as the potential energy surfaces produced in this work, is available as [Supporting Information](#).

■ ASSOCIATED CONTENT

■ Supporting Information

The Supporting Information is available free of charge on the ACS Publications website at DOI: [10.1021/acs.jpca.7b10483](https://doi.org/10.1021/acs.jpca.7b10483).

CAS data (TXT)

Band origins with excited rotational levels (PDF)

MRCI data for HCN and HNC (TXT)

Fortran subroutines for the main nonrelativistic Born–Oppenheimer potential energy as well as the adiabatic and relativistic correction surfaces (ZIP)

■ AUTHOR INFORMATION

Corresponding Author

*(O.L.P.) E-mail: o.polyansky@ucl.ac.uk.

ORCID

Oleg L. Polyansky: [0000-0002-7127-3271](https://orcid.org/0000-0002-7127-3271)

Notes

The authors declare no competing financial interest.

■ ACKNOWLEDGMENTS

This work was supported by the ERC Advanced Investigator Project 267219 and the Russian Fund for Fundamental Studies (Grant 15-02-07473). We are grateful to the reviewers for many useful comments.

■ REFERENCES

- (1) Baraban, J. H.; Changala, P. B.; Mellau, G. C.; Stanton, J. F.; Merer, A. J.; Field, R. W. Spectroscopic characterization of isomerization transition states. *Science* **2015**, *350*, 1338–1342.
- (2) Mellau, G. C.; Kyuberis, A. A.; Polyansky, O. L.; Zobov, N.; Field, R. W. Saddle point localization of molecular wavefunctions. *Sci. Rep.* **2016**, *6*, 33068.
- (3) van Mourik, T.; Harris, G. J.; Polyansky, O. L.; Tennyson, J.; Császár, A. G.; Knowles, P. J. *Ab initio* global potential, dipole, adiabatic and relativistic Correction surfaces for the HCN/HNC system. *J. Chem. Phys.* **2001**, *115*, 3706–3718.
- (4) Harris, G. J.; Polyansky, O. L.; Tennyson, J. *Ab initio* spectroscopy of HCN/HNC. *Spectrochim. Acta, Part A* **2002**, *58*, 673–690.
- (5) Nguyen, T. L.; Baraban, J.; Ruscic, B.; Stanton, J. On the HCN - HNC Energy Difference. *J. Phys. Chem. A* **2015**, *119*, 10929–10934.
- (6) Barber, R. J.; Strange, J. K.; Hill, C.; Polyansky, O. L.; Mellau, G. C.; Yurchenko, S. N.; Tennyson, J. ExoMol line lists - III. An improved hot rotation-vibration line list for HCN and HNC. *Mon. Not. R. Astron. Soc.* **2014**, *437*, 1828–1835.
- (7) Barber, R. J.; Harris, G. J.; Tennyson, J. Temperature dependent partition functions and equilibrium constant for HCN and HNC. *J. Chem. Phys.* **2002**, *117*, 11239–11243.
- (8) Harris, G. J.; Pavlenko, Y. V.; Jones, H. R. A.; Tennyson, J. The identification of HCN and HNC in carbon stars: Model atmospheres. *Mon. Not. R. Astron. Soc.* **2003**, *344*, 1107–1118.
- (9) Bucher, C. R.; Lehmann, K. K. Vibrationally mediated dissociation of HCN. *Chem. Phys. Lett.* **1998**, *294*, 173.
- (10) Hu, Q. J.; Zhang, Q.; Hepburn, J. W. Threshold ion pair production spectroscopy of HCN. *J. Chem. Phys.* **2006**, *124*, 074310.
- (11) Quapp, W.; Klee, S.; Mellau, G. C.; Albert, S.; Maki, A. Fourier-transform spectra of overtone bands of HCN from 4800-cm(−1) to 9600-cm(−1) - some new transitions of bending combination-modes. *J. Mol. Spectrosc.* **1994**, *167*, 375–382.
- (12) Maki, A.; Quapp, W.; Klee, S.; Mellau, G. C.; Albert, S. The CN mode of HCN: A comparative study of the variation of the transition dipole and Herman-Wallis constants for seven isotopomers and the influence of vibration-rotation interaction. *J. Mol. Spectrosc.* **1995**, *174*, 365–378.
- (13) Maki, A.; Quapp, W.; Klee, S.; Mellau, G. C.; Albert, S. Intensity measurements of $\Delta l < 1$ transitions of several isotopomers of HCN. *J. Mol. Spectrosc.* **1997**, *185*, 356–369.
- (14) Maki, A. G.; Mellau, G. C.; Klee, S.; Winnemisser, M.; Quapp, W. High-temperature infrared measurements in the region of the bending fundamental of (HCN)-C-12-N-14, (HCN)-C-12-N-15, and (HCN)-C-13-N-14. *J. Mol. Spectrosc.* **2000**, *202*, 67–82.
- (15) Mellau, G. C.; Winnemisser, B. P.; Winnemisser, M. Near infrared emission spectrum of HCN. *J. Mol. Spectrosc.* **2008**, *249*, 23–42.
- (16) Mellau, G. C. Complete experimental rovibrational eigenenergies of HCN up to 6880 cm(−1) above the ground state. *J. Chem. Phys.* **2011**, *134*, 234303.
- (17) Mellau, G. C. The nu(1) band system of HCN. *J. Mol. Spectrosc.* **2011**, *269*, 12–20.
- (18) Mellau, G. C. Rovibrational eigenenergy structure of the [H,C,N] molecular system. *J. Chem. Phys.* **2011**, *134*, 194302.
- (19) Maki, A.; Quapp, W.; Klee, S.; Mellau, G. C.; Albert, S. Infrared transitions of (HCN)-C-12-N-14 and (HCN)-C-12-N-15 between 500 and 10000 cm(−1). *J. Mol. Spectrosc.* **1996**, *180*, 323–336.
- (20) Maki, A. G.; Mellau, G. C. High-temperature infrared emission measurements on HNC. *J. Mol. Spectrosc.* **2001**, *206*, 47–52.
- (21) Mellau, G. C. Complete experimental rovibrational eigenenergies of HNC up to 3743 cm(−1) above the ground state. *J. Chem. Phys.* **2010**, *133*, 164303.
- (22) Mellau, G. C. The nu(1) band system of HNC. *J. Mol. Spectrosc.* **2010**, *264*, 2–9.
- (23) Mellau, G. C. Highly excited rovibrational states of HNC. *J. Mol. Spectrosc.* **2011**, *269*, 77–85.
- (24) Hofmann, J. P.; Eifert, B.; Mellau, G. C. Near infrared emission spectrum of (HCN)-C-13. *J. Mol. Spectrosc.* **2010**, *262*, 75–81.
- (25) Yang, X.; Rogaski, C. A.; Wodtke, A. M. Vibrational structure of hydrogen cyanide up to 18 900 cm^{−1}. *J. Opt. Soc. Am. B* **1990**, *7*, 1835–1850.
- (26) Romanini, R.; Lehmann, K. K. Ring-down cavity absorption spectroscopy of the very weak HCN overtone bands with six, seven, and eight stretching quanta. *J. Chem. Phys.* **1993**, *99*, 6287–6301.
- (27) Hanel, R.; Conrath, B.; Flasar, F. M.; Kunde, V.; Maguire, W.; Pearl, J.; Pirraglia, J.; Samuelson, R.; Allison, L. H. M.; Cruikshank, D.; et al. Infrared observations of the saturnian system from Voyager-1. *Science* **1981**, *212*, 192–200.
- (28) Ridgway, S. N.; Carbon, D. F.; Hall, D. N. B. Polyatomic species contributing to carbon-star 3 micron band. *Astrophys. J.* **1978**, *225*, 138–147.
- (29) Ulich, B. L.; Conklin, E. K. Detection of methyl cyanide in comet-Kohoutek. *Nature* **1974**, *248*, 121–122.
- (30) Tennyson, J.; Yurchenko, S. N.; Al-Refaie, A. F.; Barton, E. J.; Chubb, K. L.; Coles, P. A.; Diamantopoulou, S.; Gorman, M. N.; Hill, C.; Lam, A. Z.; et al. The ExoMol database: molecular line lists for exoplanet and other hot atmospheres. *J. Mol. Spectrosc.* **2016**, *327*, 73–94.
- (31) Eriksson, K.; Gustafsson, B.; Jørgensen, U. G.; Nordlund, A. Effects of HCN molecules in carbon star atmospheres. *Astron. Astrophys.* **1984**, *132*, 37–44.
- (32) Harris, G. J.; Polyansky, O. L.; Tennyson, J. Opacity data for HCN and HNC from a new ab initio linelist. *Astrophys. J.* **2002**, *578*, 657–663.
- (33) Harris, G. J.; Tennyson, J.; Kaminsky, B. M.; Pavlenko, Y. V.; Jones, H. R. A. Improved HCN/HNC linelist, model atmospheres synthetic spectra for WZ Cas. *Mon. Not. R. Astron. Soc.* **2006**, *367*, 400–406.

- (34) Harris, G. J.; Larner, F. C.; Tennyson, J.; Kaminsky, B. M.; Pavlenko, Y. V.; Jones, H. R. A. A $\text{H}^{13}\text{CN}/\text{HN}^{13}\text{C}$ linelist, model atmospheres and synthetic spectra for carbon stars. *Mon. Not. R. Astron. Soc.* **2008**, *390*, 143–148.
- (35) Tsiaras, A.; Rocchetto, M.; Waldmann, I. P.; Tinetti, G.; Varley, R.; Morello, G.; Barton, E. J.; Yurchenko, S. N.; Tennyson, J.; et al. Detection of an atmosphere around the super-Earth 55 Cancri e. *Astrophys. J.* **2016**, *820*, 99.
- (36) Jørgensen, U. G.; Almlöf, J.; Gustafsson, B.; Larsson, M.; Siegbahn, P. CASSCF and CCI calculations of the vibrational band strengths of HCN. *J. Chem. Phys.* **1985**, *83*, 3034–3042.
- (37) Polyansky, O. L.; Ovsyannikov, R. I.; Kyuberis, A. A.; Lodi, L.; Tennyson, J.; Zobov, N. F. Calculation of rotation-vibration energy levels of the water molecule with near-experimental accuracy based on an *ab initio* potential energy surface. *J. Phys. Chem. A* **2013**, *117*, 9633–9643.
- (38) Kyuberis, A. A.; Lodi, L.; Zobov, N. F.; Polyansky, O. L. *Ab initio* calculation of the ro-vibrational spectrum of H_2F^+ . *J. Mol. Spectrosc.* **2015**, *316*, 38–44.
- (39) Polyansky, O. L.; Ovsyannikov, R. I.; Kyuberis, A. A.; Lodi, L.; Tennyson, J.; Yachmenev, A.; Yurchenko, S. N.; Zobov, N. F. Calculation of rotation-vibration energy levels of the ammonia molecule based on an *ab initio* potential energy surface. *J. Mol. Spectrosc.* **2016**, *327*, 21–30.
- (40) Varandas, A. J. C.; Rodrigues, S. P. J. New Double Many body expansion potential Energy Surface for Ground State HCN. *J. Phys. Chem. A* **2006**, *110*, 485–493.
- (41) Dawes, R.; Wagner, A. F.; Thompson, D. L. *Ab Initio* Wavenumber Accurate Spectroscopy: $(\text{CH}_2)\text{-C-1}$ and HCN Vibrational Levels on Automatically Generated IMLS Potential Energy Surfaces. *J. Phys. Chem. A* **2009**, *113*, 4709–4721.
- (42) Tennyson, J.; Kostin, M. A.; Barletta, P.; Harris, G. J.; Polyansky, O. L.; Ramanlal, J.; Zobov, N. F. DVR3D: a program suite for the calculation of rotation-vibration spectra of triatomic molecules. *Comput. Phys. Commun.* **2004**, *163*, 85–116.
- (43) Tajti, A.; Szalay, P. G.; Császár, A. G.; Kállay, M.; Gauss, J.; Valeev, E. F.; Flowers, B. A.; Vázquez, J.; Stanton, J. F. HEAT: High accuracy extrapolated *ab initio* thermochemistry. *J. Chem. Phys.* **2004**, *121*, 11599–11613.
- (44) Császár, A. G.; Allen, W. D.; Schaefer, H. F., III In pursuit of the *ab initio* limit for conformational energy prototypes. *J. Chem. Phys.* **1998**, *108*, 9751–9764.
- (45) Werner, H.-J.; Knowles, P. J.; Knizia, G.; Manby, F. R.; Schütz, M. Molpro: a general-purpose quantum chemistry program package. *WIREs Comput. Mol. Sci.* **2012**, *2*, 242–253.
- (46) Szalay, P.; Müller, T.; Gidofalvi, G.; Lischka, H.; Shepard, R. Multiconfiguration Self-Consistent Field and Multireference Configuration Interaction Methods and Applications. *Chem. Rev.* **2012**, *112*, 108.
- (47) Polyansky, O. L.; Alijah, A.; Zobov, N. F.; Mizus, I. I.; Ovsyannikov, R.; Tennyson, J.; Szidarovszky, T.; Császár, A. G.; et al. Spectroscopy of H_3^+ based on new high accuracy global potential energy and dipole moment surfaces. *Philos. Trans. R. Soc., A* **2012**, *370*, 5014–5027.
- (48) Meyer, W.; Botschwina, P.; Burton, P. *Ab initio* calculations of near-equilibrium potential and multipole moment surfaces and vibration frequencies of H_3^+ and its isomers. *J. Chem. Phys.* **1986**, *84*, 891.
- (49) Tarczay, G.; Császár, A. G.; Klopper, W.; Quiney, H. M. Anatomy of relativistic energy corrections in light molecular systems. *Mol. Phys.* **2001**, *99*, 1769–1794.
- (50) Pyykkö, P.; Dyall, K. G.; Császár, A. G.; Tarczay, G.; Polyansky, O. L.; Tennyson, J. Lamb shift effects in rotation-vibration spectra of water. *Phys. Rev. A: At., Mol., Opt. Phys.* **2001**, *63*, 024502.
- (51) Stein, C. J.; Reiher, M. Automated Selection of Active Orbital Spaces. *J. Chem. Theory Comput.* **2016**, *12*, 1760–1771.
- (52) Sayfutyarova, E. R.; Sun, Q.; Chan, G. K.-L.; Knizia, G. Automated construction of molecular active spaces from atomic valence orbitals. *J. Chem. Theory Comput.* **2017**, *13*, 4063–4078.
- (53) Rishi, V.; Perera, A.; Bartlett, R. J. Assessing the distinguishable cluster approximation based on the triple bond-breaking in the nitrogen molecule. *J. Chem. Phys.* **2016**, *144*, 124117.
- (54) Piecuch, P.; Kucharski, S. A.; Kowalski, K. Can ordinary single-reference coupled-cluster methods describe the potential energy curve of N_2 ? The renormalized CCSDT(Q) study. *Chem. Phys. Lett.* **2001**, *344*, 176–184.
- (55) Chan, G. K.-L.; Sharma, S. The Density Matrix Renormalization Group in Quantum Chemistry. *Annu. Rev. Phys. Chem.* **2011**, *62*, 465–481.
- (56) Eriksen, J. J.; Lipparini, F.; Gauss, J. Virtual orbital many-body expansions: A possible route towards the full configuration interaction limit. *J. Phys. Chem. Lett.* **2017**, *8*, 4633–4639.
- (57) Zimmerman, P. M. Strong correlation in incremental full configuration interaction. *J. Chem. Phys.* **2017**, *146*, 224104.
- (58) Tubman, N. M.; Lee, J.; Takeshita, T. Y.; Head-Gordon, M.; Whaley, K. B. A deterministic alternative to the full configuration interaction quantum Monte Carlo method. *J. Chem. Phys.* **2016**, *145*, 044112.
- (59) Liu, W.; Hoffmann, M. R. iCI: Iterative CI toward full CI. *J. Chem. Theory Comput.* **2016**, *12*, 1169–1178.
- (60) Booth, G. H.; Thom, A. J. W.; Alavi, A. Fermion Monte Carlo without fixed nodes: A game of life, death, and annihilation in Slater determinant space. *J. Chem. Phys.* **2009**, *131*, 054106.
- (61) Rolik, Z.; Szabados, Á.; Surján, P. R. A sparse matrix based full-configuration interaction algorithm. *J. Chem. Phys.* **2008**, *128*, 144101.
- (62) Martin, J. M. L. *Ab initio* total atomization energies of small molecules - towards the basis set limit. *Chem. Phys. Lett.* **1996**, *259*, 669–678.
- (63) Feller, D.; Peterson, K. A.; Dixon, D. A. The impact of Larger Basis sets and explicitly correlated coupled cluster theory of the Feller-Peterson-Dixon composite method. *Annu. Rep. Comput. Chem.* **2016**, *12*, 47.
- (64) Feller, D.; Peterson, K. A.; Hill, J. G. On the effectiveness of CCSD(T) complete basis set extrapolations for atomization energies. *J. Chem. Phys.* **2011**, *135*, 044102.
- (65) Feller, D. Benchmarks of improved complete basis set extrapolation schemes designed for standard CCSD(T) atomization energies. *J. Chem. Phys.* **2013**, *138*, 074103.
- (66) Stanton, J. F.; Gauss, J.; Harding, M. E.; Szalay, P. G.; Auer, A. A.; Bartlett, R. J.; Benedikt, U.; Berger, C.; Bernholdt, D. E.; Bomble, Y. J. et al. *CFOUR, a quantum chemical program package*; 2010; For the current version see: <http://www.cfour.de>.
- (67) Tennyson, J.; Barletta, P.; Kostin, M. A.; Polyansky, O. L.; Zobov, N. F. *Ab initio* rotation-vibration energy levels of triatomics to spectroscopic accuracy. *Spectrochim. Acta, Part A* **2002**, *58*, 663–672.
- (68) Schwenke, D. W. Beyond the potential energy surface: *Ab initio* corrections to the Born-Oppenheimer approximation for H_2O . *J. Phys. Chem. A* **2001**, *105*, 2352–2360.
- (69) Shirin, S. V.; Polyansky, O. L.; Zobov, N. F.; Barletta, P.; Tennyson, J. Spectroscopically determined potential energy surface of H_2^{16}O up to $25\,000\text{ cm}^{-1}$. *J. Chem. Phys.* **2003**, *118*, 2124–2129.
- (70) Shirin, S. V.; Zobov, N. F.; Ovsyannikov, R. I.; Polyansky, O. L.; Tennyson, J. Water line lists close to experimental accuracy using a spectroscopically determined potential energy surface for H_2^{16}O , H_2^{17}O and H_2^{18}O . *J. Chem. Phys.* **2008**, *128*, 224306.
- (71) Scherrer, A.; Agostini, F.; Sebastiani, D.; Gross, E. K. U.; Vuilleumier, R. On the Mass of Atoms in Molecules: Beyond the Born-Oppenheimer Approximation. *Phys. Rev. X* **2017**, *7*, 031035.
- (72) Herman, R. M.; Asgharian, A. Theory of energy shifts associated with deviations from Born-Oppenheimer behavior in $^1\Sigma$ -state diatomic molecules. *J. Mol. Spectrosc.* **1966**, *19*, 305.
- (73) Bunker, P. R.; Moss, R. E. Breakdown Of Born-Oppenheimer Approximation - Effective Vibration-Rotation Hamiltonian For A Diatomic Molecule. *Mol. Phys.* **1977**, *33*, 417–424.
- (74) Pachucki, K.; Komasa, J. Nonadiabatic corrections to the wave function and energy. *J. Chem. Phys.* **2008**, *129*, 034102.

- (75) Lodi, L.; Tennyson, J.; Polyansky, O. L. A global, high accuracy ab initio dipole moment surface for the electronic ground state of the water molecule. *J. Chem. Phys.* **2011**, *135*, 034113.
- (76) Carter, S.; Mills, I. M.; Handy, N. C. Vibration-rotation variational calculations - precise results on HCN up to 25000 cm⁻¹. *J. Chem. Phys.* **1993**, *99*, 4379–4390.
- (77) Boyarkin, O. V.; Koshelev, M. A.; Aseev, O.; Maksyutenko, P.; Rizzo, T. R.; Zobov, N. F.; Lodi, L.; Tennyson, J.; Polyansky, O. L. Accurate bond dissociation energy of water determined by triple-resonance vibrational spectroscopy and ab initio calculations. *Chem. Phys. Lett.* **2013**, *568–569*, 14–20.
- (78) Morley, G. P.; Lambert, I. R.; Ashfold, M. N. R.; Rosser, K. N.; Western, C. M. Dissociation dynamics of HCN(DCN) following photoexcitation at 121.6 nm. *J. Chem. Phys.* **1992**, *97*, 3157.
- (79) Cook, P. A.; Langford, S. R.; Ashfold, M. N. R.; Dixon, R. N. Angular resolved studies of the Lyman- α photodissociation of HCN and DCN: new dynamical insights. *J. Chem. Phys.* **2000**, *113*, 994.
- (80) Rolik, Z.; Szegedy, L.; Ladóczki, B.; Kállay, M.; et al. An efficient linear-scaling CCSD(T) method based on local natural orbitals. *J. Chem. Phys.* **2013**, *139*, 094105. See also www.mrcc.hu.
- (81) Kállay, M.; Szalay, P. G.; Surján, P. R. A general state-selective multireference coupled-cluster algorithm. *J. Chem. Phys.* **2002**, *117*, 980–990.
- (82) Irikura, K. K. Experimental vibrational zero point energies: diatomic molecules. *J. Phys. Chem. Ref. Data* **2007**, *36*, 389.
- (83) Prasad, C. V. V.; Bernath, P. F. Fourier transform jet-emission spectroscopy of the A ²Π_i → X ²Σ⁺ transition of CN. *J. Mol. Spectrosc.* **1992**, *156*, 327.
- (84) Knowles, P. J.; Hampel, C.; Werner, H.-J. Coupled cluster theory for high spin, open shell reference wave functions. *J. Chem. Phys.* **1993**, *99*, 5219. Knowles, P. J.; Hampel, C.; Werner, H.-J. Erratum: "Coupled cluster theory for high spin, open shell reference wave functions". *J. Chem. Phys.* **2000**, *112*, 3106.
- (85) Watts, J. D.; Gauss, J.; Bartlett, R. J. Coupled-cluster methods with noniterative triple excitations for restricted open-shell Hartree-Fock and other general single determinant reference functions. Energies and analytical gradients. *J. Chem. Phys.* **1993**, *98*, 8718.
- (86) Ruscic, B.; Pinzon, R. E.; Morton, M. L.; von Laszewski, G.; Bittner, S. J.; Nijsure, S. G.; Amin, K. A.; Minkoff, M.; Wagner, A. F. Introduction to Active Thermochemical Tables: Several "Key" Enthalpies of Formation Revisited. *J. Phys. Chem. A* **2004**, *108*, 9979–9997.
- (87) Maksyutenko, P.; Muenter, J.; Zobov, N.; Shirin, S.; Polyansky, O. L.; Rizzo, T. R.; Boyarkin, O. Approaching the full set of energy levels of water. *J. Chem. Phys.* **2007**, *126*, 241101.
- (88) Grechko, M.; Maksyutenko, P.; Zobov, N.; Shirin, S.; Polyansky, O.; Rizzo, T.; Boyarkin, O. Collisionally Assisted Spectroscopy of Water from 27 000 to 34 000 cm⁻¹. *J. Phys. Chem. A* **2008**, *112*, 10539–10545.
- (89) Grechko, M.; Boyarkin, O. V.; Rizzo, T. R.; Maksyutenko, P.; Zobov, N. F.; Shirin, S.; Lodi, L.; Tennyson, J.; Császár, A. G.; Polyansky, O. L. State-selective spectroscopy of water up to its first dissociation limit. *J. Chem. Phys.* **2009**, *131*, 221105.
- (90) Császár, A. G.; Mátyus, E.; Lodi, L.; Zobov, N. F.; Shirin, S. V.; Polyansky, O. L.; Tennyson, J.; et al. Ab initio prediction and partial characterization of the vibrational states of water up to dissociation. *J. Quant. Spectrosc. Radiat. Transfer* **2010**, *111*, 1043–1064.